An-Najah National University

Faculty of Graduate Studies

CONTROL STRATEGY AND OPERATING LIMITS OF PHOTOVOLTAIC INVERTER SUPPORTING THE MAIN GRID BASED ON VIRTUAL SYNCHRONOUS GENERATOR CONCEPT

By

Noor Aldeen Basem Ghazzawi

Supervisors

Dr. Moien A. Omar

Prof. Marwan M. Mahmoud

This Thesis is Submitted in Partial Fulfillment of the Requirements for the Degree of Master Electrical Power Engineering, Faculty of Graduate Studies, An-Najah National University, Nablus - Palestine.

2022

CONTROL STRATEGY AND OPERATING LIMITS OF PHOTOVOLTAIC INVERTER SUPPORTING THE MAIN GRID BASED ON VIRTUAL SYNCHRONOUS GENERATOR CONCEPT

By

Noor Aldeen Basem Ghazzawi

This thesis was defended successfully on 17/04/2022 and approved by

Dr. Moien A. Omar	______________________
Supervisor	Signature
Prof. Marwan M. Mahmoud	______________________
Co-Supervisor	Signature
Dr. Jaser A. Saed	______________________
External Examiner	Signature
Dr. Tamer Khatib	______________________
Internal Examiner	Signature

Dedication

إلى من بلّغ الرسالة ونصح الأمّة ..... إلى خير البريّة وسيّد ولد آدم؛ سيّدنا محمّد عليه الصلاة والسلام.

إلى الذي رأيت الفخر بعينيه، إلى الذي تعب لأرتاح وسهر لأنام، إلى قرّة العين ونبض الفؤاد، إلى أبي رحمه الله ورزقه الفردوس الأعلى.

إلى التي وصّانا عليها رسول الله صلّى الله عليه وسلّم، إلى من تحت قدميها الجنّة، إلى أمّي حفظها الله وبارك لها في عمرها.

إلى كلّ من جاد عليّ بعلمه وخبرته، إلى كلّ من جعلني أحبّ العلم وأسلك طريقه، إلى أساتذتي الأفاضل حفظهم الله ونفع بهم.

إلى رفاق الدّرب، إلى إخوتي وأصدقائي وأحبائي.

إلى الشهداء والأسرى.

أهدي هذه الأطروحة إليكم جميعا، والله من وراء القصد.

Acknowledgments

First and foremost, I would like to express my sincere thanks to Allah for empowering me and giving me the ability to finish this work successfully.

Many sincere thanks to my supervisors Dr. Moien Omar and Dr. Marwan Mahmoud who have helped me with their experience and knowledge to complete this work.

Special thanks to Dr. Moien Omar who motivated and supported me during searching and writing this thesis. My thanks also to the staff and colleagues of the Electrical Power Engineering Master Program at An Najah national University.

I extend my sincere thanks to the discussion committee for accepting the discussion of this thesis.

Finally, I would like to thank all of the people who helped me in some way during writing this thesis.

Declaration

I, the undersigned, declare that I submitted the thesis entitled:

CONTROL STRATEGY AND OPERATING LIMITS OF PHOTOVOLTAIC INVERTER SUPPORTING THE MAIN GRID BASED ON VIRTUAL SYNCHRONOUS GENERATOR CONCEPT

I declare that the work provided in this thesis, unless otherwise referenced, is the researcher's own work, and has not been submitted elsewhere for any other degree or qualification.

Student's Name: ______________________________

Signature: ______________________________

Date: ______________________________

List of Contents

List of Tables

List of Figures

List of Appendices

CONTROL STRATEGY AND OPERATING LIMITS OF PHOTOVOLTAIC INVERTER SUPPORTING THE MAIN GRID BASED ON VIRTUAL SYNCHRONOUS GENERATOR CONCEPT

By
Noor Aldeen Basem Ghazzawi
Supervisor
Dr. Moien Omar
Prof. Marwan Mahmoud

Abstract

This thesis presents a control scheme of virtual synchronous generator in photovoltaic inverters without using external energy storage systems, where instead the reserve active power is used to improve the grid frequency as well as the grid voltage. The reserve power concept is possible in the smart grid context because some of the power inverters are smart inverters and all are controlled by a control unit. The grid operator can reduce the output power from these inverters in the case the power generated from the inverters is more than the power required by the load. Meanwhile, the active power can be reduced or increased even without using external storage which is with high investment cost. The case study includes a PV inverter with a rated power of 50 kVA, a PV system with a rated power of 50 kW, and a grid voltage of 380 V. When the solar radiation was 200 W/m^2, and the load power was 120 kW, 37.5 kVAr, the load voltage was 202.4 V. The proposed control strategy improved the voltage by 17.6 V to be 220V. When the solar radiation was 1000 W/m^2, and the load power was 20kW, 7.5kVAr, the load voltage was 230V. The proposed control reduced the voltage by 10 V to be 220 V. When there was a variable frequency of ±0.4 Hz from the nominal frequency of 50 Hz, the proposed control improved the frequency by ±0.4 Hz to be 50 Hz.

In the case of low load voltage (204 V) with a rise in system frequency (50.2 Hz), the proposed control strategy improved the voltage by 15V to be 219 V and improved the frequency by reducing the output power of the PV system by 4kW.

The MATLAB/SIMULINK software was used to simulate and to show the effectiveness of the proposed control strategy to improve system stability with different scenarios.

Keywords: virtual synchronous generator, distributed generation, high penetration, frequency stability, voltage stability, power reserve control.

Chapter one

Introduction and Theoretical Background

1.1 General Introduction

The concept "Traditional power plant" describes generating electricity from oil, coal, or natural gas [1].

The installation and operation of these power plants can have environmental effects such as CO2 emissions, nuclear waste, and a large amount of water used in these power plants [2]; So, as a result, it's necessary to find a sustainable and environmentally acceptable energy source.

In the last few years, there is a high demand on power plants which use renewable energy sources (RESs), solar and wind energy are the two most famous sources [3]; for example, in 2020, 14.1 GW is generally linked to the electrical grid, and by 2030 the amount is expected to increase to 53 GW [4]. The interest in this type of energy production comes back for several reasons, including the growth of popularity of clean energy and the positive environmental effects of these clean energy sources compared with the traditional sources. In addition, because of the significant change in the field of power electronics during the last decades. This increase in the capacity of renewable energy sources causes an up normal conditions to the electrical grid [3, 5].

1.2 Problem statement

High penetration levels of distributed generation systems of renewable energy sources connected to the grid through power electronics converters have a significant impact on the grid stability. And this refers to the characteristics of these power converters that suffer from the lack of rotating mass which is the source of inertia and damping properties that help to enhance grid stability [6-8].

However, high penetration levels pose a risk to grid stability and affects the dynamic performance of the grid. Among these negative effects are voltage fluctuation, increasing power loss and harmonics, reverse power flow and protection problems [2, 9].

Several studies have been published to reduce these effects. The best solution to mitigate these problems which was achieved by using the Smart inverters [2]. Recently, Virtual

Synchronous Generators (VSGs) will present an appropriate idea for controlling the power inverters in power systems [6].

VSG control will expect to act as a synchronous generator in providing more damping properties and virtual inertia for the inverter to enhance grid stability [10-12].

1.3 Motivation

The generator that is commonly used in the traditional power plants is the synchronous generator (SG) [1]. SG has many features such as its rotating mass and damping properties, its ability to control the reactive power flow that regulates the voltage in the grid, and the grid frequency, which is vital to hold out the grid dynamics and ensure grid stability [5, 8].

However, due to the natural variations of RES distributed generation, ensuring grid stability and a power balance with energy production and demand is extremely difficult [6, 13, 14].

Photovoltaic systems that are connected to the network through the inverters, which convert the generated DC power to AC power should have some of the following capabilities: provide or absorb active and reactive power, voltage ride-through, voltage/frequency control for islanding mode [15, 16].

Voltage fluctuations are the major power quality issues related to fast PV output variations or sudden changes in loads. These fluctuations can destroy electrical appliances linked to the network and compromise grid stability [6, 13].

All the reasons have been mentioned were the motivation for this study which focuses on control the inverters to support developing of PV systems in the utility grid.

1.4 Objectives

1.4.1 General objective

The objective of this study is to develop a control strategy for a three-phase grid-connected inverter that emulates the inertia and damping properties of the synchronous generator, with droop controllers and current control strategies without using the energy storage systems, where the current command will be provided by a VSG model.

1.4.2 Specific objectives

The main goals of this study are as follows:

1- Provide a control plan for the traditional synchronous generator, in which the automatic voltage regulator (AVR) control regulates the output voltage and the governor control to maintain system frequency.

2- Investigate and design the power electronics control techniques to emulate the behavior of traditional synchronous generators.

3- Provide a control design to implement and simulate the proposed control strategy for grid-connected inverters.

4- Study the current VSG methods, evaluate the implementation and construction of the system, and discover the range and constraints.

1.5 Thesis outlines

This thesis consists of five chapters:

Chapter 1: Introduce the assumption of this thesis, which contains an outline of the constraints and issues associated with the effect of the high penetration level of a renewable energy system in the grid.

Chapter 2: Give basic information on power systems that use conventional synchronous generators, such as stability and inertia properties and introduce a review of the existing methods that emulate the synchronous generator's behavior to compare the new methods.

Chapter 3: Explain and present the traditional control scheme of the grid-connected inverter, also illustrate the frequency response techniques.

Chapter 4: Explains and models the suggested control technique, the virtual synchronous generator control, without using the energy storage systems.

Chapter 5: Introduce the simulation results of the proposed control strategy in grid mode and the simulation results of multi-cases that include variable irradiations and loads. Show the effects of high penetration levels of renewable energy distributed generations on grid stability and Illustrate the results, as well as the constraints of the proposed control strategy, and present recommendations for future studies.

Chapter Two

Power system stability and Virtual Synchronous Generator topologies

2.1 Introduction about traditional and modern power systems

Power systems subdivided into two systems: the traditional power system and the modern power system. The definition and difference between these system presented in the following sections.

2.1.1 Traditional power systems

A Conventional power system has a central station that will produce electrical power and transmit it from the generating unit to the different loads; it also connects the station with transmission lines and distribution systems. Traditional power stations use non-renewable energy sources such as fossil fuels, which consist of coal and oil used in most of these stations and considered the primary energy source that controls the turbine.

In general, traditional power systems consists of generating substations, transformers, transmission systems, distribution systems, and different types of loads.

Synchronous generators are the most machines used in traditional power systems, these SGs have many characteristics; the most important are:

- Inertia because of the rotating mass.
- Damping property due to the damper winding.
- Droop control for load sharing.

There are two-control loops that are used in the traditional stations:

The first is the automatic load frequency control (ALFC), which controls frequency variation to keep the active power stable in the system. It's accurate while there is a small and slow change in loads and divided into two functions [17]:

1- The primary ALFC, its principal functions are to keep the frequency constant, regulate the flow of the tie-lines, and distribute the loads across the participating generation units. According to the frequency and power deviations, the valve position changed, and the prime mover varies its active power to perform active power balance according to this position.
2- The second loop of ALFC or the supplementary loop can restore the frequency to the reference value by using an integral controller that makes the deviation of the

frequency equal to zero and provides a reasonable adjustment based on the characteristic of the power-frequency droop curve.

The second is the automatic voltage regulator that controls reactive power by controlling the generator field current, hence regulating the terminal voltage [17].

Moreover, these characteristics are not available in traditional power converters.

2.1.2 Modern Power Systems

Smart grid is an example of modern power system. It is a modernized version of the conventional power system that offering safe and reliable operation because there is an advanced communication between the utility and the consumer. The modern power system can analyze and control grid-connected operations and offer real information on all occurrences.

Other technical developments such as distributed RESs, energy storage systems, modern communication systems, and electric vehicle charging stations are all part of the modern power systems, as shown in figure A.1 in appendix A [18].

2.2 Power systems stability

Power systems are made of different synchronous machines (SMs) which works in synchronism. It is important for power system's stability that they maintain good synchronism under all situations, and the system generates a force that causes it to return to the normal or the stable condition when a disturbance arises in the system, and the ability of different machines in the network to stay in synchronism after any disturbance with each other is called power system stability [7, 18, 20].

2.3 Classification of power system stability

There is different classification of power system stability, as shown in figure A.2 in appendix A, depending on the next factors [7]:

- Nature and type of the disturbance.
- Disturbance size.
- Duration of the fault.

There are different forms of disturbance in the power system, such as a change in load gradually or suddenly, faults of all types of symmetrical and asymmetrical fault, loss of switching operation, etc.

Different types of stability in the power system had been categorized to facilitate the process of identifying the reasons for instability and provide solutions to improve system stability according to these reasons.

According to figure A.2 in appendix A, problems of power system stability can be categorized as follows:

- Rotor angle stability.
- Frequency stability (in small and high range).
- Voltage stability.

Each type of stability can be subdivided as follow [21]:

- Dynamic or steady-state stability (small signal): the electric power system expects to remain stable after slow and small disturbance. This type of stability is called Steady State Stability.
- Transient stability: after a large disturbance like a fault in transmission lines or a sudden large change in load, the faulted part could be separated from the rest of the network, so that leads to a structural change of the power system, and this type of stability is called Transient Stability.
- First swing stability: the period under investigation is one or a fraction of seconds following a system failure (based on a basic model of the generator).
- Multi swing stability: the period under investigation is about ten seconds after a system fault (based on the advanced model of the generator, and it must consider the impacts of the control model).

The objective of all stability studies is to determine if the electric power systems after a following disturbance are back to a steady-state operation or not.

2.3.1 Voltage stability

In the previous section, voltage stability is one of the important types of power system stability. Recently, voltage stability issues have happened continuously, so it’s important to study this type of stability because the voltage problems may effects the stability in all power systems [22, 23].

The majority of recent faults that happened in the power system were caused by the instability in system voltage. For example, the blackout accident that happened in some areas in Canada grid, which continued for almost a week and it was the cause of load losses estimated at 62,000 MW in 2003 and the blackout that happened in China and Ningxia, which lead to load losses reached to 480 MW, 420 MW in years 1989, 1995 respectively [22, 24, 25].

Some of the reasons for rising voltage instability problems are as follows:

- Environmental protection pressures when building the generating plants and developing lines.
- Increasing consumption of electricity.
- Increasing distributed generation units which use renewable energy sources in the system.

There are many definitions for voltage system stability. According to Chinese Standard DL 755-2001 titled “The safety and stability standards for power grids” the definition of voltage system stability is the capability of the system to regulate the grid voltage in an appropriate and reliable range after a different disturbance appears in the grid such as lines failures, increasing or decreasing load demands, tripping of the producing units. Also, the normal and up-normal operation conditions are put forwards [22].

According to IEEE and CIGRE38 groups, The other definition is “that every node in the grid can keep the voltages in appropriate range after disturbances appear in a certain operation state and depend on the balance between the load demand and source in the power grid” [7].

The issue is not easy and simple when talking about reactive power balancing as it is when talked about active power. In each node in the grid and according to Kirchhoff’s first current rule, there must be a balance between the generated and absorbed reactive power. And based on the amount of injected reactive power, the desired voltage is normally regulated [26].

In fault cases, the generated reactive power is generally so tiny. So, the voltage level in this case, cannot be maintained to appropriate levels.

2.3.2 Frequency stability

According to IEEE and CIGRE38 research groups, the definition of system frequency stability is “the capability of the system to keep the operation of the power system in steady-state frequency after the disturbance such as unbalance between the load demand and the generation appears in the grid” [27]. Therefore, it is important to study this type of stability to balance electricity consumption and generation.

The many problems that happened in the power system were appeared by the instability in system frequency. For example, some of the transmission lines (380 kV) were removed from the service because of the drop in the frequency, which led to a blackout in Italy in 1994. In the same year, another blackout happened in Australia because the system frequency drops at 3.5 Hz per sec [27].

The system frequency has directly related to the active power that can be absorbed or produced in the grid, and based on the injected active power; the system frequency can be controlled [21].

2.4 Swing equation

Several SMs formed the power system, and these machines operate under all operational scenarios. The equation that described the relationship between the electromagnetic torque and the input of mechanical torque and considered as the heart of the electric power system is called the Swing Equation, and it’s as follow [16, 17]:

$$T_m(t) - T_e(t) = D\frac{d\delta(t)}{dt} + J\frac{d^2\delta(t)}{dt^2} \tag{2.1}$$

Where

J: is the moment of inertia.

δ: is the angular difference between the rotor’s angular position and the reference position.

D: is the factor of damping.

Tm: is the mechanical or shaft torque.

Te: is the electromagnetic torque.

These values are in function of t (time in second).

The inertia property of SG reacts to the disturbance and consider a vital part of system stability, that's the most important feature of SMs [7, 17].

2.5 Improve power system stability

In the power systems, there are several methods to improve the voltage and frequency stability in the grid, such as: increasing the output of the swing and other generators in the network up to 10% 5% of nominal power, respectively, increasing or decreasing tab changer of transformers in the network and can be used the capacitors bank and shunt reactors, then developing these methods by FACT devices such as Static Synchronous Series Compensator (SSSC), Static Compensator (STATCOM), Static Synchronous Series Compensator (SSSC) [18, 21].

Domestic loads and low-voltage energy sources are integrated into the grid. Hence, the presence of several DG units that connect to the grid through the power converters causes many problems to the electrical network, such as stability issues and voltage fluctuations because of the lack of inertia in power converters and the dependence on climate fluctuations that solved via the applications of smart inverters instead of traditional inverters such as the effective VSG control technology. VSG gives inertia and damping effects to the inverter like the standard SM with the proper control strategy, which helps to ensure grid stability.

2.6 Voltage and Frequency standards

The main aim of this approach is to explain and clarify the supply voltage characteristics about the magnitude and the frequency. These characteristics vary during regular supply system operation due to changes in load, and the development of failures mainly caused by external occurrences.

The nominal frequency and voltage in low voltage supply must be 50 Hz, 230 V, respectively. The average value of the frequency recorded over 10 s under typical operating conditions must be within the range of (47-52) Hz, and the mean value of the voltage all 10 min must be within the range of (195.5-253) V according to the EN50160 standard [28].

2.7 Virtual Synchronous Generator topologies

VSG control strategy was found in 2007 as a technique of solving stability issues in the grid caused by the high integration of RESs [10, 29]. Different research projects are still experimenting with different models and control systems to imitate the behavior of traditional SGs, as presented in previous sections.

There are two types of control for applying VSG's concept: the VSG with energy storage and VSG without energy storage.

Several research groups in VSG with energy storage type are searching on virtual synchronous generators, and the most important groups are as follows:

1. The first VSG topology proposed by the Institute of Electrical Power Engineering research group in Germany (IEPE).
2. The second VSG topology proposed by the INGENIA Solar Energy group at Osaka University (ISE).
3. The third VSG topology proposed by the Kawasaki Heavy Industries research group (KHI).
4. The fourth VSG topology proposed by the VSYNC group.

And in the VSG without energy storage type as the virtual synchronous generator with power reserve control projects (VSG_PRC).

2.8 Concept of virtual synchronous generator

Previous sections presented a virtual synchronous generator as a possible solution to the electrical grid stability issues caused by the increase of the penetration levels of RES in the network. A VSG will form by three special components: a power electronic converter, an energy storage system, and the appropriate control technique.

Figure A.3 shows the general structure of VSG, a distributed generation of RES unit connected to the electrical grid through the inverter. It is supposed to work equally to normal SG by providing virtual inertia and damping properties and having the same reaction as the SG when a sudden load change or any disorder happens in the network.

The VSG block can determine and regulate the inverter's output power depending on the rate of change in grid frequency and voltage, and the difference between the reference values of voltage and frequency with the grid values, similarly to how traditional SGs are controlled [8].

2.9 Virtual synchronous generator topologies with energy storage systems

In this type of control, the research groups depend on the energy storage systems to provide additional inertia. So, when the grid needs to a large amount of active power bigger than the PV system can produce, the energy storage system can provide this amount of active power to the grid. Also, if we need to reduce the active power in the grid, the energy storage system will absorb this active power to improve the system's operation. Short overview of these methods will be presented in the following sections.

- The first topology

The Institute of Electrical Power Engineering research group at CLAUSTHAL University in Germany created a VSG model, commonly known as a virtual synchronous machine (VISMA). There are two ways for VISMA implantation, which are VISMA-method1 and VISMA-method2 [30-33].

- VISMA-method1

The main concept of the VISMA model is that a block control representing a synchronous algorithm will provide a reference value of voltage or current depending on the grid measurements [30, 32], and figure 2.1.a shows the overview of VISMA-method1

Figure 2.1.a shows the overview of the VISMA-method1. The VISMA model will begin with real-time grid voltage measurements that provide the virtual synchronous algorithm block (VSA). The VSA block will generate the reference current and rotational angle and activate the inverter switches via the hysteresis controller.

The inertia and damping features of SM could be modified by varying the parameter of the VSA model, and the stator current is represented by the following equations to determine the reference value of current [32]:

$$i_1 \cdot R_s + L_s \cdot \frac{di_1}{dt} = e_1 - v_1 \tag{2.2}$$

$$i_2 \cdot R_s + L_s \cdot \frac{di_2}{dt} = e_2 - v_2 \tag{2.3}$$

$$i_3 \cdot R_s + L_s \cdot \frac{di_3}{dt} = e_3 - v_3 \tag{2.4}$$

Representation in vectors is as follow:

$$I_{ref}^{\rightarrow} \cdot R_s + L_s \cdot \frac{dI_{ref}}{dt} = e^{\rightarrow} - v^{\rightarrow} \tag{2.5}$$

Where

$e^{\rightarrow} = [e_1 e_2 e_3]^T$ **:** is the induced electromotive force in the stator (EMF).

$v^{\rightarrow} = \begin{bmatrix} v_1 \\ v_2 \\ v_3 \end{bmatrix}$: is the grid voltages.

R_s , L_s : are the resistance and inductance of stator.

So according to equation (2.5), the reference current in the Laplace domain can be determined as

$$I_{ref}^{\rightarrow}(s) = \frac{e^{\rightarrow}(s) - V_{grid}^{\rightarrow}(s)}{L_s.s + R_s} \tag{2.6}$$

The rotor dynamic is represented by the following equations [32]:

$$T_{mech} - T_{elec} = \frac{1}{J} . \frac{dw}{dt} + K_d . f(s) . \frac{dw}{dt} \tag{2.7}$$

$$\begin{cases} T_{elec} = \frac{P_{elec}}{w} \\ \theta = \int w . dt \end{cases} \tag{2.8}$$

Where

$T_{mech.}$, $T_{elec.}$: are the mechanical and electrical torque.

J: is the inertia.

K_d: is the factor of damping.

w, θ: are the angular velocity and the rotational angle respectively.

f(s): is the phase compensation term which use to ensure that the virtual damping power is counteractive to any rotor action in the opposite phase.

Finally, the EMF as a function of theta can be written as [32] :

$$e = \begin{bmatrix} e_1 \\ e_2 \\ e_3 \end{bmatrix} = E_p \, . \begin{bmatrix} \sin(\theta) \\ \sin(\theta - \frac{2}{3} \, . \, \pi) \\ \sin(\theta + \frac{2}{3} \, . \, \pi) \end{bmatrix} \tag{2.9}$$

Where E_p is adjustable amplitude to give the induced EMF.

A mathematical VSA model can be represented based on the equations (2.2) to (2.9) as illustrated in figure 2.1.b.

Figure 2.1.a

The structure of VISMA-method1 [31]

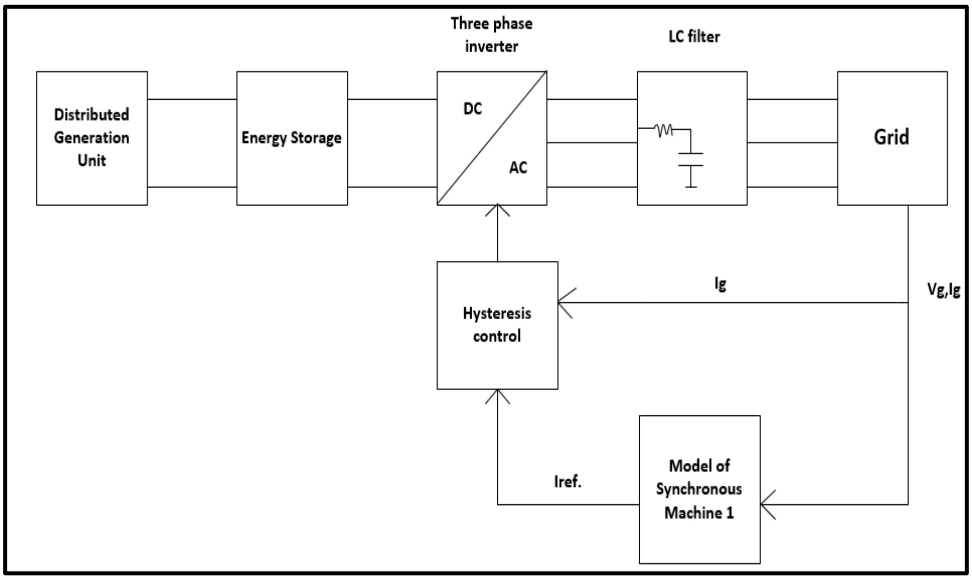

Figure 2.1.b

Visma-method1 block diagram [31].

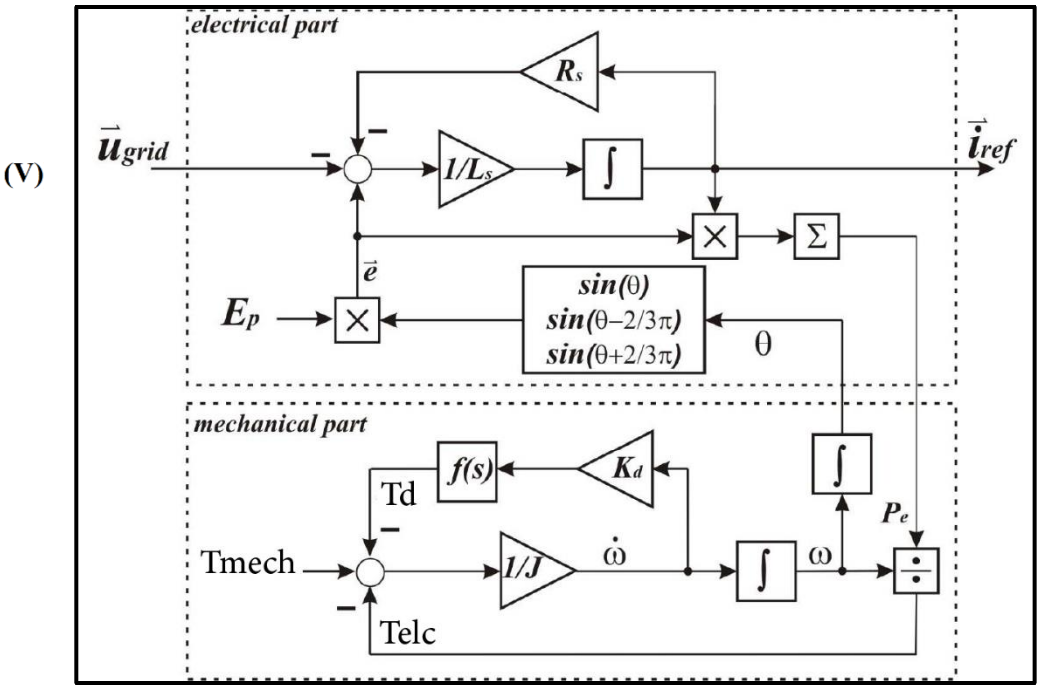

- VISMA-method2

VISMA-method2 is another approach created by the IEPE group. In this method, the grid current is used as an input to the VSA block and will generate a reference voltage as an output to energize the inverter switching by using a pulse width modulation controller

(PWM) instead of the hysteresis controller as in the VISMA-method1, to use a constant switching frequency which makes it easy to select the filter circuit [31].

The overview model of VISMA-method2 and the mathematical representation of the VSA block are shown in figures 2.2.a and 2.2.b.

Figure 2.2.a

The structure of VSG VISMA-method2 [31].

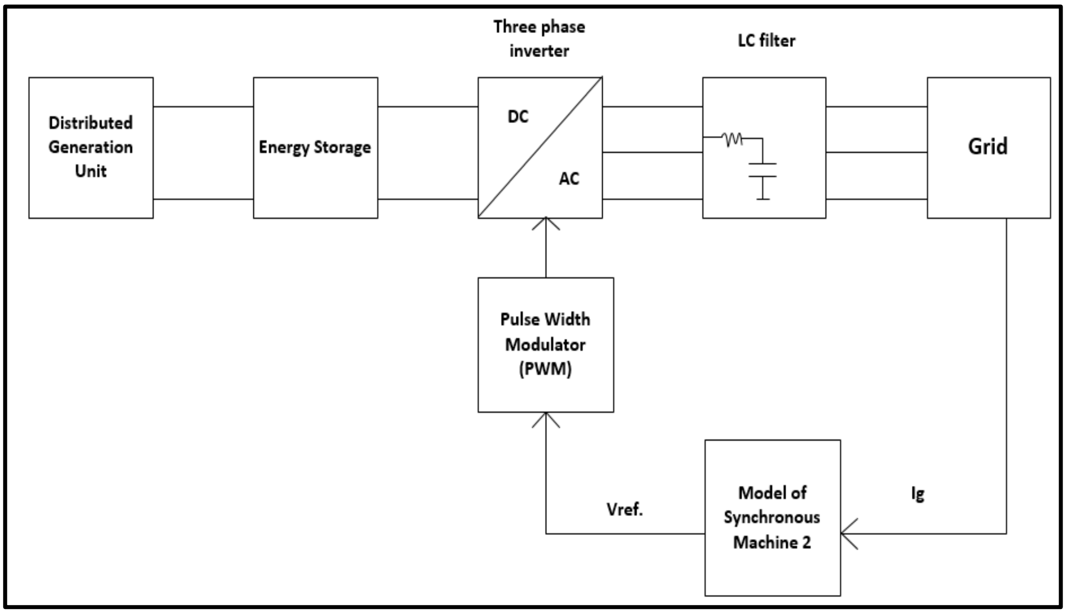

Figure 2.2.b

Visma-method2 block diagram [31].

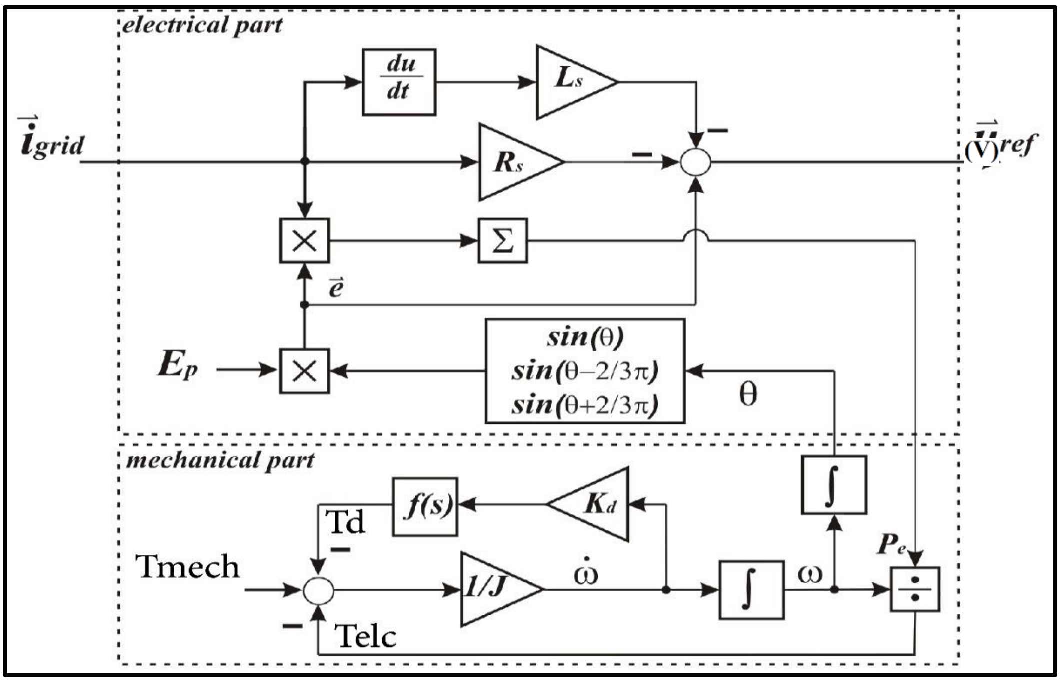

In island mode, the two methods can be activated, but the VISMA-mehod2 is better than VISMA-method1 for improving voltage quality, and it's easier to use [31].

- The second topology

In 2011, The INGENIA Solar Energy group at Osaka University in Japan developed a new strategy control of VSG, commonly known as the ISE-VSG, as illustrated in figure A.4 [11, 34-37]:

In this design, a cylindrical rotor type of SG was used, and the VSG control block is used to provide a mechanical phase angle depending on the swing equation, which is expressed by the next equation [11]:

$$P_{in} - P_{out} = D\Delta\omega_m + Jw_m \frac{dw_m}{dt} \tag{2.10}$$

$$w_m = \frac{d\theta_m}{dt} \tag{2.1}$$

Where

P_{in} : is the turbine power to SM and it represents the input power.

P_{out}: is the grid power that represents the out power of VSG.

J , D , Wm , θ_m : are the inertia, the damping factor, the speed of the rotor, and the mechanical phase angle, respectively.

In this model, the voltage and current are measured on the grid side, and by using a power meter block, the active output power (P_{out}) could be determined. Also, the frequency can be measured by using a phase-locked loop block. By setting the reference input power Pin depending on the relation between input power and output power of VSG as shown in equation (2.12), the VSG block will give (w_m) virtually and by applying the integration on this(w_m), will provide virtual (θ_m) as the first input to PWM . By choosing the voltage reference as the second input, the PWM will generate pulses for energizing the inverter switching and deliver the proper power depending on the grid condition.

$$P_{in} = K_p * \Delta w + K_i * \frac{\Delta w}{dt} + K_{soc} * \Delta soc \tag{2.12}$$

Where

K_p , K_i , K_{soc} : are damping, dimensionless, state of charge factors, respectively.

➢ The third topology

In 2012, The Kawasaki Heavy Industries research group developed a VSG controller depending on the algebraic model of SG by using the phasor diagram to generate a current reference to guarantee the necessary operation under all types of load, and the structure of the KHI model is illustrated in figure A.5 [38].

In this model, they use a governor control model to generate the load angle (δ). By setting the reference real power as the first input, then through a droop control gain with reference angular velocity, they get on the δ .

To produce the internal electromotive force of the generator (E_f), they use the automatic voltage regulator (AVR) control model by setting the reference reactive power as the second input. Through a droop control gain with a reference voltage and feedback signal of terminal voltage (Vg) via PI controller, they get on the E_f.

The reference current will be generated depending on the phasor diagram of the SG shown in figure A.6 by using the E_f,δ and Vg.

The reference current (I^*) can be determined using equations 2.13 and 2.14. Furthermore, this reference current controls the PWM to generate pulses for driving the inverter.

This type of control could be used in grid mode and island mode, and it can operate under unbalanced loads depending on the current controller. Also, this control supports the parallel operation in island mode.

$$\begin{bmatrix} I_d^* \\ I_q^* \end{bmatrix} = Y\begin{bmatrix} E_d \\ E_q \end{bmatrix} - Y\begin{bmatrix} V_{g_d} \\ V_{g_q} \end{bmatrix} = \frac{1}{r^2+x^2}\begin{bmatrix} r & x \\ -x & r \end{bmatrix}\left(\begin{bmatrix} E_d \\ E_q \end{bmatrix} - \begin{bmatrix} V_{g_d} \\ V_{g_q} \end{bmatrix}\right) \tag{2.13}$$

$$\begin{cases} Y = \frac{1}{r^2+x^2}\begin{bmatrix} r & x \\ -x & r \end{bmatrix} \\ \begin{bmatrix} E_d \\ E_q \end{bmatrix} = \left|\dot{E}_f\right|\begin{bmatrix} \sin\theta \\ \cos\theta \end{bmatrix} \end{cases} \tag{2.14}$$

Where

r: is the virtual resistance.

x: is the virtual reactance.

Y: is the admittance matrix.

➢ The fourth topology

Figure A.7 illustrates the topology of VSG control established by the VSYNC group [10, 12].

The energy source is connected to the main grid through a power electronic inverter and filter circuit to provide a virtual inertia property to the system. Using the PLL block, the frequency of the grid, the rate of change in frequency, and the reference signal of frequency will be measured.

P and Q on the output of the inverter can be calculated by using state of charge of energy storage (SOC), deviation of frequency, reference frequency, grid voltage, and the reference voltage depending on the following equation [5]:

$$\begin{cases} P = K_p * \Delta w + K_i * \frac{\Delta w}{dt} + K_{soc} * \Delta soc \\ Q = \Delta v * K_v \end{cases} \tag{2.15}$$

According to the next two equations, the reference current used to deliver the PWM to generate the pulses for the inverter can be calculated as follow :

$$\begin{cases} i_d = \frac{(v_d * P - v_q * Q)}{(v_d + v_q)^2} \\ iq = \frac{(v_d * Q + v_q * P)}{(v_d + v_q)^2} \end{cases} \tag{2.16}$$

Where

P, Q: are output active and reactive power of VSG control respectively.

v_d , v_q: are the voltage in dq frame.

i_d , i_q: are the reference current in dq frame.

2.10 Virtual synchronous generator topologies without energy storage systems

This method is indicated by the symbol “VSG_PRC“. It is a new method that appeared in 2019 by the research group at the Lanzhou University of Technology in China.

In this system, they depend on the concept of power reserve control instead of depending on the energy storage systems to improve the system frequency stability as in the traditional methods. In another way, the PV system can preserve an amount of real power-up or down-regulation capability in actual time by reducing the output power of PV systems in a specific range [39].

This method will be used in our thesis. The following chapters will discuss the operation of the PV system with the virtual synchronous generator by using power reserve control in detail.

Chapter Three

The control of grid-connected PV system

3.1 Introduction

Chapter 2 shows several topologies, and different types of VSG control strategies with energy storage devices responsible for providing inertia property to the inverter also illustrates the concept of operating with active and reactive power.

According to the analysis, the improvement goals are to support the main grid and ensure voltage system stability based on the grid conditions and load type.

The fundamental structure and construction of traditional control of the grid inverter utilized in this research is provided in this chapter.

The principal objective of this study is to consider grid-connected solar distributed generations, which is a very important and popular model, and several test situations have been examined to assess the suggested system that uses PV arrays as the voltage source. Firstly, a short overview of the PV inverter and the traditional control scheme of the grid-connected inverter is presented. Secondly, a general overview of the whole system is presented, and then the relevant mathematical model explaining each element that emulates the proposed control is discussed.

3.2 PV inverter

Solar energy is one of the famous sources of renewable energy [2], and the photovoltaic panel is one of the necessary components in solar system. The power generated from PV panels is DC power, and the power usually is used for domestic and industrial loads in the grid is AC-grid. So the PV system is connected to the load via the inverter, a power electronics device have been used to transform the power from DC power to AC power to the loads, and all modern power systems do not be without it [40].

There are several classifications of inverters: islanding inverters, grid-tie inverters, and hybrid inverters. When an inverter have been selected, it should have many properties, including efficiency curve, special internal protection, scalability, DC and AC voltage standards, etc. [41].

This study will focus on grid inverters due to the large use of this type of inverters. Grid inverter requires to be synchronized with the grid. With a proper control mechanism, the inverter can deliver or absorb the proper active and reactive power depending on the grid conditions for achieving more system stability [40].

Grid-tie inverters techniques in solar systems usually comprise different types of micro-inverters, string, and centralized inverters. Micro-inverters connect every panel to its single inverter, and micro-inverters provide maximum power optimization but it is more expensive than the other two types [42].

In a central inverter, power plants that generate a huge amount of power ranging from 500 kW to 2.5 MW, every power block at the power plant will be equipped with a single central inverter. However, string inverters utilize a distributed system instead of a centralized one, so every section of the PV array will be with a small inverter, and the benefit of this type is that when any inverter fails, only that section of the PV array will be lost compared to the whole system in the central inverter and the next table shows a comparison between central and string inverters [43].

Table 3. 1:

General comparison between string and central inverters

String inverters	Central inverters
Distributed structure	Centralized construction
Small physical and with low nominal power.	Physically bigger and with greater nominal power.
Low voltages and simple to service	High voltages and hard to service
Less cost per Watt	High cost per Watt

3.3 Traditional control of grid-tie inverters

Grid inverters must be synchronized with the grid to make the system more stable and reliable. The requirements for controlling the grid inverters are as follows [22]:

- Ability to control the active power in two directions.
- Ability to control reactive power independently in the two directions.
- DC-voltage control to keep the voltage at the proper levels.

The inverter used in this thesis is a two-stage inverter. The first stage is the DC/DC converter to control the DC voltage and provide the maximum power to the next stage by using the Maximum Power Point Tracking control (MPPT). The second stage is the DC/AC inverter to provide the all-active power that can be generated from the PV arrays by using the DC link voltage control, current control, vector oriented control (VOC), and control of synchronization, as shown in figure A.8.

3.4 The concept of maximum power point tracking control

To regulate the inverter output power at any time, notably during varying solar radiation, and to study the naturally low efficiency of the solar panels, the maximum power point tracking control is used. The main significant benefit of using MPPT control is its capability to detect the maximum power point (MPP) as effectively as possible. Many various MPPT methods are available to find the best voltage and current values of the PV panel to achieve the highest output power level depending on the Voltage-Current characteristic of the PV panel, as shown in figure A.9 [44, 45].

As shown in figure A.9, there is a three-point on the curve: point A is the top of the figure, and point C is the bottom, nevertheless, neither is the maximum power point. Point B is the MPP located between the A and the B points because it has the highest output power, which is 224 W.

3.5 Technologies for grid synchronization

Earlier, they synchronize the inverter with the grid by repeating the grid voltage in a way to keep the reference of output current and the grid voltage in the same phase [46].

In recent years, they used the phase-locked loop for grid inverter synchronization (PLL). PLL is a control system used to extract the phase angle from grid voltage and used this angle in the system control [47]. The primary function of PLL is to follow the voltage and frequency of the grid, where the phase voltage of inverter output be in phase with the phase voltage of the main grid in the case of grid synchronization.

In this study, the synchronous reference frame phase-locked loop is used to achieve the objective mentioned above. Figure A.10 shows the internal structure of the PLL block, which consists of three main blocks: PI controller to provide a fast dynamic response, voltage-controlled (VCO) to generate a sinusoidal signal, and a phase detector [48].

As shown in figure A.10, the phase detector detected the input signal frequency and compared it with the output signal frequency of VCO. Then, if there is a difference between these two signals, the error signal will be generated and filtered by using a PI controller to control the VCO frequency.

3.6 Current control

In a three-phase inverter, there are two methods for the control: current control and voltage control.

The current control method is used to control the output active and reactive power by regulating the current injected in the main grid. On the other hand, the voltage control controls the power flow by using the phase shift between the output voltage of the inverter and the grid voltage.

The output of power electronic inverter should be sinusoidal, and its frequency and magnitude can be regulated, so it has been needed to control the current responsible for this operation. The current controller helps to enhance the power quality by offering over-current protection and providing compensation for the harmonics [50]. There are several methods for the current controller: hysteresis controller, PI current controller, and predictive current controller.

This thesis uses the linear PI current controller since it has a low total harmonic distortion (THD), fast dynamic response and low sensitivity of other current controllers [51].

According to the filter circuit diagram, the current controller that supports the implementation of the current control block has been designed [52].

Figure A.11 shows the circuit diagram of the LCL filter. The reason to choose this type of filter on other types such as L and LC filter is because it has a better performance to reduce the harmonics in the grid, excellent in reducing inverter switching frequency harmonics, and decreases the filter's dependency on the parameter of the main grid.

The LCL filter is assumed to be lossless. Then, by applying Kirchhoff's voltage low on figure A.11, the next equations can represent the LCL filter [53]:

$$\begin{cases} L_{1,filter}.\frac{dI_{in}}{dt} = V_{in} - V_c \\ L_{2,filter}.\frac{dI_g}{dt} = V_c - V_g \end{cases} \tag{3.1}$$

Where

V_{in}: is the output voltage of the inverter.

V_c: is the voltage across the filter capacitor.

V_g: is the grid voltage.

$L_{1,filter}$, $L_{2,filter}$: are inductance filters.

The currents and voltages in this equation rotate at the same synchronous speed W_{syn}, and can be transformed the above equations from natural reference frame control (ABC frame) to the synchronous rotating frame (DQ control) by using Park's transformation as follow:

$$L_{1,filter}.\frac{dI_{in,d}}{dt} = V_{in,d} - V_{c,d} + w_{syn}.L_{1,filter}.I_{in,q} \tag{3.2}$$

$$L_{1,filter}.\frac{dI_{in,q}}{dt} = V_{in,q} - V_{c,q} - w_{syn}.L_{1,filter}.I_{in,d} \tag{3.3}$$

$$L_{2,filter}.\frac{dI_{g,d}}{dt} = V_{c,d} - V_{g,d} + w_{syn}.L_{2,filter}.I_{g,q} \tag{3.4}$$

$$L_{2,filter}.\frac{dI_{g,q}}{dt} = V_{c,q} - V_{g,q} - w_{syn}.L_{2,filter}.I_{g,d} \tag{3.5}$$

$$C_{filter}.\frac{dV_{c,d}}{dt} = I_{g,d} - I_{in,d} + w_{syn}.C_{filter}.V_{c,q} \tag{3.6}$$

$$C_{filter}.\frac{dV_{c,q}}{dt} = I_{g,q} - I_{in,q} + w_{syn}.C_{filter}.V_{c,d} \tag{3.7}$$

In the above equations, the fact that the (d) and (q) axis currents and voltages are coupled can be seen, and we should remove this coupling to improve the performance of regulation, then make the output current follows the reference current.

The coupling can be eliminated by using a PI controller and feed-forward control, which is a decoupling control in the current controller. The PI controller is also used to make the output current follows the reference current. The current controller takes the following form:

$$\begin{cases} V_{in,d} = V_{g,d} - w_s . L . I_{in,q} + K_p\left(i_{in,d_{ref}} - i_{in,d}\right) + K_i \int (i_{in,d_{ref}} - i_{in,d}) \\ V_{in,q} = V_{g,q} + w_s . L . I_{in,d} + K_p\left(i_{in,q_{ref}} - i_{in,q}\right) + K_i \int (i_{in,q_{ref}} - i_{in,q}) \end{cases} \tag{3.8}$$

The previous two equations generated the reference voltage in the d-q reference frame for the outer system. Using inverse Park's transformation, the reference voltage in the d-q frame will transform to reference voltages in the ABC frame, which are used as a primary control for the PWM control block to control the inverter by generating the pulses that regulate the output power of the inverter [54].

Figure A.12, shows the internal structure of the current controller, in which k_p is the proportional gain and k_i is the integral gain of the PI controller.

In traditional control of grid inverter, the reference current Id_{ref} fed from the DC-link voltage control and the Iq_{ref} equal to zero, which means the inverter will work at unity power factor (PF).

3.7 DC-Link voltage control

Based on operational environmental situations, such as ambient temperature and solar irradiation, the DC link voltage fluctuates between two different levels and makes unbalance between the DC and AC powers. So, this type of control is used to keep the DC-link voltage at the appropriate voltage.

The next equations express the active and reactive powers of the inverter in the d-q frame [55]:

$$P = \frac{3}{2} * (V_{g_d} . i_d + V_{g_q} . i_q) \tag{3.9}$$

$$Q = \frac{3}{2} * (V_{g_d} . i_d - V_{g_q} . i_q) \tag{3.10}$$

$$P_{dc} = V_{dc} . I_{dct} \tag{3.11}$$

Where

P: is active power on the AC side.

Q: is the reactive power on the AC side.

V_{dc}: is the voltage across the dc-link capacitor.

I_{dct}: is the current in the DC terminal of the inverter.

The (V_{g_q}) is zero and the (V_{g_d}) is the rated voltage (V_g) during the operation in steady-state, because the d-q components of grid voltages are constant at the rated values. According to the previous assumption, the equations P and Q will be as follow:

$$\begin{cases} P = \frac{3}{2}\, V_g.\, i_d \\ Q = \frac{3}{2}\, V_g.\, i_d \end{cases} \tag{3.12}$$

And if we neglect the losses in the DC/DC and DC/AC converters, the power on the DC side will be equal with the power on the AC side, so,

$$P_{DC\_side} = P_{AC\_side} \tag{3.13}$$

Then,

$$\mathrm{Vdc.\,Idct} = \frac{3}{2}\, V_g.\, i_d \tag{3.14}$$

According to equation (3.14), if there is any change in the power balance between the DC and AC sides, the voltage of the DC capacitor will change. PI controller will produce the reference current ($i_d{}^*$) according to the error between the actual DC-link voltage, and the reference voltage as shown in figure A.13. And this reference current will be used to keep the voltage at the appropriate value.

3.8 Frequency response techniques for PV systems

There are two categories for the frequency response (FR) [56]:

1- By using energy storage.

2- By applying the power reserve control.

The first, PV integrated with short-term energy storage such as batteries, which provides the inertia for the power electronic inverter and provide the power reserve from the energy storage system. There are many strategies for controlling the PV-storage grid system. Such of them, the energy storage system developed an MPPT control and the three-phase inverter using a VSG control, and they both can deliver inertial and main frequency support for micro-grids [57] or a genetic algorithm can be used to study the response of the frequency and its stability by improving the parameter values for VSG control but this method its very complicated [58]. However, there are many problems when energy storage is used, like the high cost of the batteries and in some regions, the energy storage systems cannot extensively be utilized because the efficiency of charge and discharge is low and this refers to the limitations of the current energy storage systems level in high penetration level of PV power plants as in Hexi New Energy Base in China [39].

The second is power reserve control or the de-load control incorporates frequency response into the PV system itself, there are several strategies that have been presented for PV systems. For example, in [59], presents an algorithm for tracking the maximum power to operate the PV systems under or below the maximum power point, and in [60] an adaptive flexible power tracking was suggested to speed up the monitoring process. However, this thesis uses the measurements of solar irradiations and temperatures with applying the direct power control for tracking the maximum power as will present in the following chapter.

Chapter Four

The proposed control scheme of virtual synchronous generator

4.1 Overview of the proposed system

The overview of grid-connected PV systems and the configuration of control power is show in figure A.14. This grid-connected system's major energy source is the PV arrays that generate DC voltage, as seen in the figure's left upper corner. The PV system is connected to a DC/DC converter then connected to a power electronics inverter, which converts the DC power into AC power at 50 Hz frequency.

The proposed control is subdivided into two control loops: Control the DC/DC converter depending on the power reserve concept, and implement VSG control to drive the inverter's output power that must be supplied or absorbed from the main grid to improve voltage profile and support system frequency stability. The other side of the inverter or the output of the inverter is connected to the main grid through a filter circuit, an LCL filter type, to minimize the harmonics and optimize the output signal form.

In the proposed control strategy, as shown in figure A.14, three-phase voltage and current on the grid side were measured and transformed from abc frame to dq frame by using Park's transformation, which is a way to simplify the calculations and enables the system to regulate the d and q axis independently. Then calculates the active, reactive power, and frequency on the grid side. Also uses these values as input signals in the VSG and PRC control blocks to provide the proper active and reactive power for supporting the grid.

The reference current Id_{ref} is fed from the DC-voltage control according to the PRC regulations, and the Iq_{ref} is fed according to the proposed Q-V droop control.

4.2 Reactive power-Voltage droop control

The output voltage of the synchronous generator is directly connected to the reactive power delivered by SG, and figure A.15 shows the reactive power-voltage droop controller that is used to perform the voltage stability.

According to figure A.15 and equation (4.1), the required reactive power that regulates the load voltage to be 220 V (PH-N) can be determined. Then compare this value with the available reactive power of the inverter can provide or absorb.

$$Q_{req} = \frac{Q_{max}}{0.08 * V_{nom}} * (v_{nom} - v_{mes}) \tag{4.1}$$

Where

Q_{req}: is the required reactive power that is needed to regulate the voltage.

Q_{ava}: is the available reactive power the inverter can supply or absorbed.

v_{nom}: is the nominal AC voltage.

v_{mes}: is the voltage measured on the grid side.

There is a limitation for reactive power which can be noticed in figure A.15, and this limitation is to protect the grid from the reverse power flow that causes several problems like the over-voltage, also there is another limitation concern to the available reactive power in the inverter according to the next cases:

$$Q_{ref} = \begin{cases} Qm_{ava} & , \; Q_{req} > Qm_{ava} \\ Q_{req} & , \; -Qm_{ava} < Q_{req} < Qm_{ava} \\ -Qm_{ava} & , \; Qreq < -Qm_{ava} \end{cases} \tag{4.2}$$

$$Qm_{ava}^2 = S_{inv}^2 - P_{inv}^2 \tag{4.3}$$

Where

Q_{req}: is the required reactive power before the comparison with the available reactive power, and it is the output of the Q-V droop control block.

Q_{ref}: is the required reactive power after comparing it with the available reactive power.

Qm_{ava}, $-Qm_{ava}$: are the maximum and minimum of available reactive power, respectively.

Then by using equation (4.4), we can determine the required reference current for the current controller block. This current block calculates the reference voltage of three phases for PWM. Furthermore, the PWM will generate pulses to control the inverter to provide the proper reactive power. The flowchart of this part of the control is shown in Figure 4.1.

$$IQ_{ref} = Q_{ref} / (\sqrt{\frac{3}{2}} * V_{3\theta}) \tag{4.4}$$

Figure 4.1

Flowchart of reactive power control

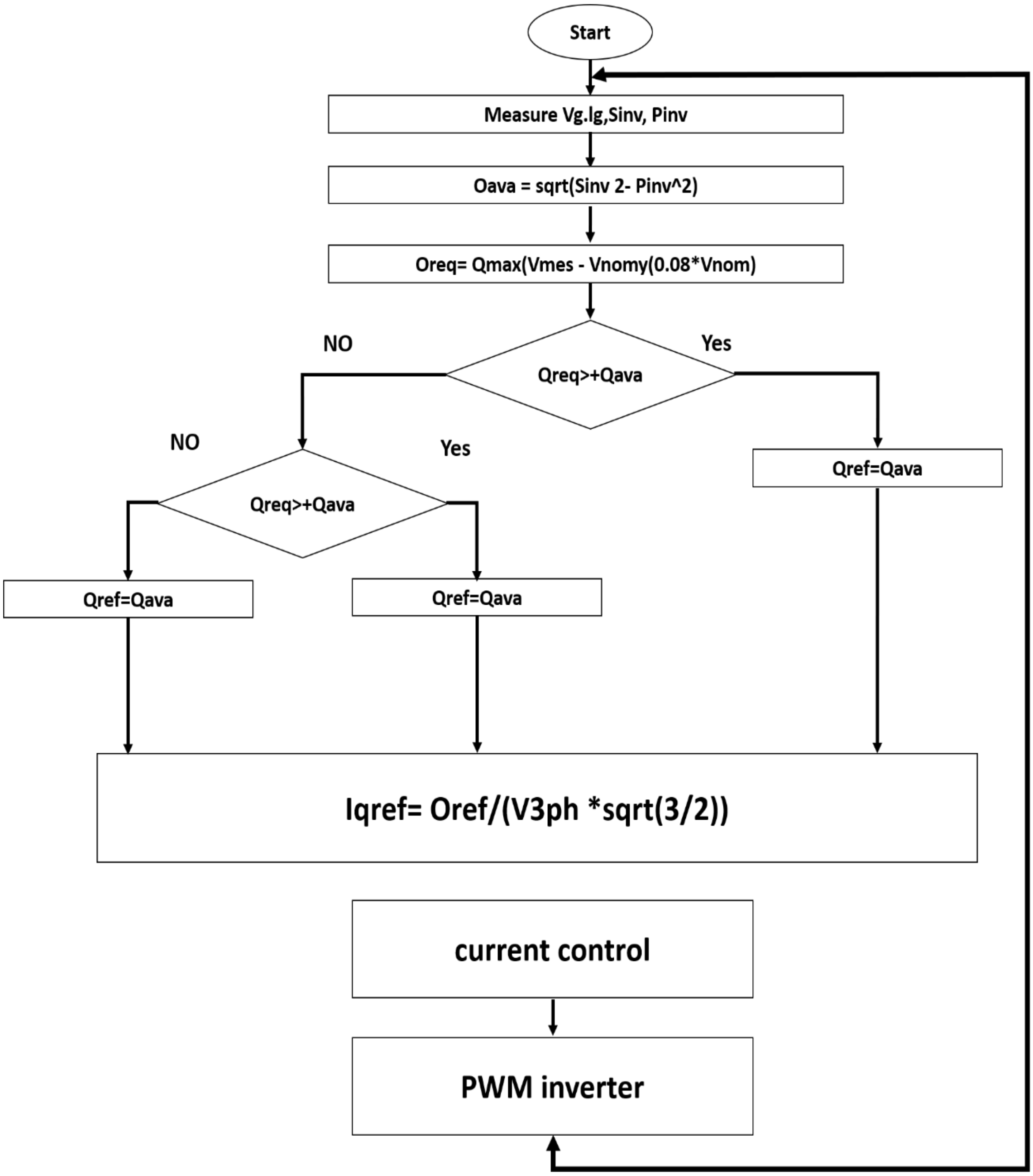

4.3 The proposed VSG with power reserve control

Power reserve control or the de-load power control is a technique that is used in traditional generators to keep the power between the generation and the demand balanced. The goal of this method is to keep the system within the nominal range of frequency and voltage. PV systems will reduce the output power of the PV system and reserve a certain amount of active power for grid suppuration according to the next equation [56].

$$P_{mpp} = P_{de-load} + \Delta P \tag{4.5}$$

Where

P_{mpp}: is the maximum power point.

$P_{de-load}$: is the output power generated from the PV system when operating in PRC mode.

ΔP: is the amount of reserve real power of PV system.

4.3.1 Analysis of voltage operating point:

Figure A.16 shows the characteristic curve of output Power-Voltage of PV module, and there are two different operating points of voltage in the non-maximum power point can be noticed. Equation (4.6) shows the relation between these different operating voltages V_a, V_b and Vmpp , also it shows that the same reserve power is installed in power reserve control mode.

$$\begin{cases} \mathrm{Vb} > \mathrm{Vmpp} > \mathrm{Va} \\ |\mathrm{Vmpp} - \mathrm{Va}| = \Delta\mathrm{Va} > \Delta\mathrm{Vb} = |\mathrm{Vmpp} - \mathrm{Vb}| \end{cases} \tag{4.6}$$

Where

ΔVa: is the voltage regulation on the Va side.

ΔVb: is the voltage regulation on the Vb side.

In this thesis, the inverter doesn't operate at Vmpp because the output power in the mpp area will be uncontrollable power. So we left with two sides, the Va side and the Vb side.

Figure A.17, shows the output power of PV in different solar radiations with a 10% reserve power of Pmpp. Also it can be seen that the Vb side has a steeper slope than on the Va side and the Vb side has a faster response because the voltage regulation on the Vb side is smaller than on the Va side.

Where

V_{in}: is the minimum input voltage of the inverter to work effectively and normally.

V_{out} : is the maximum input voltage of the inverter to work safely and normally.

$P_{de-load1}$, $P_{de-load2}$: are the output power when PRC operates in Va & Vb side respectively.

P_{mpp}: is the maximum power in MPPT mode.

However, if the system runs in MPPT or PRC mode, the possibility of the inverter operating safely and effectively when connected to the grid must be taken into account. Therefore, every inverter has a certain workspace where it can work normally, and it can be get it from the datasheet of the inverter.

For example, in figure A.17, if the output voltage of the PV system in the inverter workspace range [Vin - Vout], the inverter will work safely and effectively, and there are three situations to inverter work:

1- The PRC mode operates on the V_{mpp}.
2- The PRC mode operates on the Va side.
3- The PRC mode operates on the Vb side.

As it was mentioned before, the PRC mode will not operate on the V_{mpp} area because the output power cannot be regulated. If the PRC mode operates on the Va side, there are some different points where the inverter will not work normally and will go to shut down. Like when the solar radiations changes from (600 to 300) W/m^2 because the output voltage of PV will be smaller than the Vin of the inverter.

On the other hand, when the PRC operates on the Vb side, the inverter will work normally and effectively in each operating point with different solar radiation because the output voltage of PV going to be within the range of the inverter workspace.

So, for keeping the ability to control the output of the inverter and to ensure that the inverter is working in safe and reliable operation, the ideal area for the inverter when the PRC operates on Vb side.

In this thesis, as shown in figure A.18, the voltage in PRC mode is always greater than the voltage in MPPT mode. This proves that the inverter will always continue in the Vb side to achieve better performance including the accurate and reliable operation of the inverter.

4.3.2 Maximum power point estimation.

According to equation (4.5), the current P_{mpp} will be a known value. Therefore, there is an additional block, the MPPE block, which is the maximum power point estimation block necessary to operate in PRC mode and to estimate the P_{mpp}.

There are several methods to implement the MPPE block. In case of using, the estimation method presented in [61] that will be used. It is based on taking two similar groups of PV modules of the same quantity and the same model. Then when working under the same operational conditions, PV1, which is the first group of the PV system operating in MPPT mode and can be utilized its output power as the exciting power of the second group of the PV system (PV2), in another way (P_{mpp} for PV1 = P_{mpp} for PV2) as shown in figure A.19.

The research group in [61]; maintained the output power of PV by controlling the output voltage, but this method needs to exhaust control procedure.

In this thesis the method presented in [39], which uses the direct power control to regulate the output power of PV as shown in figure A.19, will be considered. By using this method, the PRC will operate within the Vb side and reduce the input current of the inverter.

4.3.3 Power reserve control with frequency support and reserve ratio analysis:

The Reserve ratio represents the percentage of power that the inverter will reserve and this value can be calculated according to the next relation [56]:

$$R_p = \frac{\Delta p}{p_{mpp}} * 100\% \tag{4.7}$$

In PRC mode, a portion of the PV system's power up-regulation ability is retained, allowing the PV system's output to be modified within a certain range, and reserve power regulation has the same effect as charging and discharging the energy storage system, and the real output power can be adjusted. According to VSG control, the participating active power and the frequency support can be realized by applying the power-frequency (P-f) droop equation. The output power needed can be represented as shown in equation (4.8).

$$P_{fs} = \frac{P_{max}}{0.01 * Fnom.} * (F_{nom} - F_{mes}) \tag{4.8}$$

Where

R_p **:** is the reserve power ratio.

P_{fs}: is the reference power for frequency support.

F_{mes}: is the frequency measured.

F_{mes}: is the nominal frequency.

The P-f droop equation controls the generator frequency dynamics. If there is a change in the grid frequency, P_{fs} will change, and the inverter will support the grid with the appropriate power. Figure A.20, shows the droop control between the power supplied by the SG and the frequency to perform the frequency stability of the system.

4.4 Power Reserve Regulations

The operation mode of PRC in the PV system is incompatible with the good use of energy and with the national codes applicable because of the abandonment of some PV resources. Anyway, due to the benefits of using the VSG with PRC mode method of improving the grid stability, reducing the system cost because the ESSs are not used in this method, and improving the power grid's adoption of PV energy.

Therefore, It is important to use the proposed method to maintain part of the PV output power in a certain amount, which is called the reserve power for grid, and this power in actual operation is mostly limited by the next factors [39].

1- According to relevant State Energy Administration rules in China, to fix the issue of clean energy consumption, the reserve power will not exceed of 10% of the PV maximum power.
2- During low solar radiation, the reserve power will be zero.
3- The PV with VSG control will be allowed to participate the power to support the grid in FR when:
a- The output power of PV is 20% of rated power and more.
b- The deviation of frequency is greater than (±0.03 Hz) which is the frequency dead zone.

4- limitation for participating the power, the top limit of real power can be raised at most to 10% of Pmpp, and the 20% of Pmpp is the maximum limit of real power that can be reduced.

According to the previous factors, there is a limitation of giving up part of PV power for participating in FR. So, when the system frequency increased, the ΔP will be increased and the maximum value for increasing ΔP is 30% of Pmpp. But when the system frequency decrease less than the nominal frequency, the ΔP will be decreased and the maximum value for this decreasing is 10% of Pmpp as shown in equation (4.9)

$$\Delta P_{ref} = \begin{cases} 30\%\ \mathrm{Pmpp}\,, & P_{fs} < -20\%\ \mathrm{Pmpp} \\ \Delta P - P_{fs}\,, & -20\%\ \mathrm{Pmpp} \leq P_{fs} \leq \Delta P \\ 0\,, & P_{fs} \geq \Delta P \end{cases} \tag{4.9}$$

Which the ΔP_{ref} is the reference reserve power during principal FR.

The flowchart of the grid frequency support is shown in figure 4.2, and the proposed control mentioned in this chapter will be simulated in the following chapter.

Figure 4.2

Flowchart of active power control.

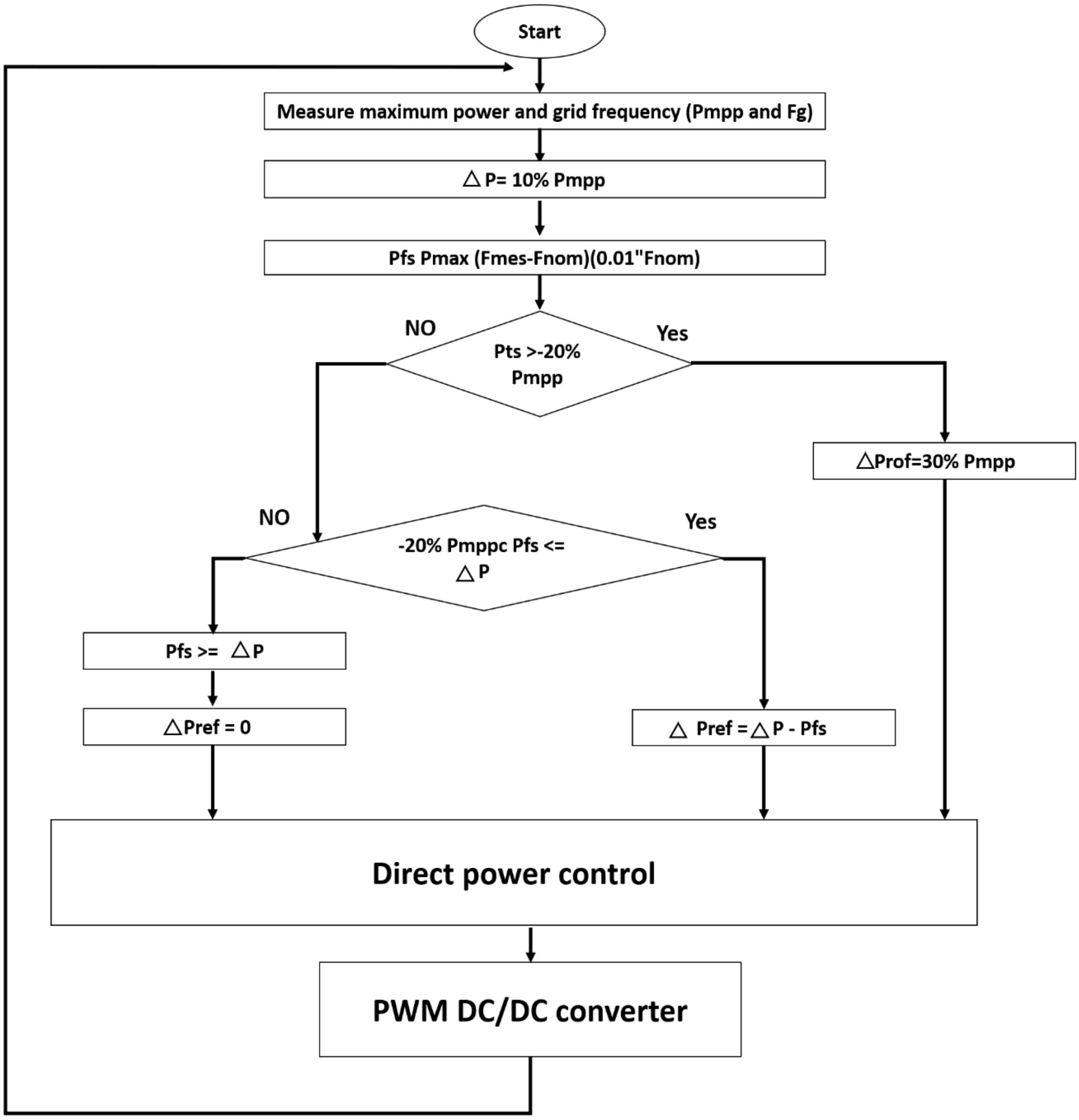

Chapter Five

Simulation results of different scenarios and conclusion

This chapter provides multi-test scenarios to examine the suggested VSG with power reserve control. The simulation studies that given in chapter 5 are built by using MATLAB/SIMULINK software, as well as the droop gain of the droop controller for VSG control strategy was determined in chapter 5. In contrast, the gains of the PI controller were obtained by the trial and error method.

5.1 Scenarios

Many test scenarios with the proposed control strategy will be running in this thesis to check the success of the system and its opportunity to improve.

- **The first scenario: Simulation results without using the proposed control strategy**

We will implement a PV system with a rated power of 50kW through a three-phase grid inverter with a rated power of 50 kVA in this case. Then the PLL and the MPPT control are using to see and study the properties, the response, and the behavior of the inverter and the main grid under any disturbance as significant changes in load and changes in solar radiations.

- **The second scenario: Simulation results with using the proposed control strategy for voltage improvements**

In this scenario, a 50 kW PV system and a three-phase inverter were connected to the main grid by using the proposed control strategy with a low and high penetration level of the distributed generation system. Then showing the inverter's response and voltage profile improvements during the disturbances, such as unstable load voltage.

- **The third scenario: Simulation results with using the proposed control strategy for frequency improvements**

In this scenario, a 50 kW PV system and a three-phase inverter were connected to the main grid by using the proposed control strategy. Then showing the inverter's response and voltage profile improvements during the disturbances, such as the varying frequency in the grid.

- **The fourth scenario: Simulation results with using the proposed control strategy for frequency and voltage improvements**

In this scenario, a 50 kW PV system and a three-phase inverter were connected to the main grid by using the proposed control strategy. Then showing the inverter's response and voltage profile improvements during the disturbances, such as the varying frequency in the grid and unstable load voltage.

5.2 Simulation Parameters

Table 5.1 shows the parameters of PV arrays and the DC/DC converter with PRC control, grid inverter with VSG control, transmission line, and filter parameter beside the parameters of PI controllers:

Table 5. 1:

Simulation parameters

V nominal (line to line)	380 V
F nominal	50 Hz
R (transmission line)	0.015 ohm/km
L (transmission line)	(4.3263/1000) H/km
Distance	0.2 km
DC voltage	800 V
Rated power of the inverter	50 kVA
L filter	540e-6 H
C filter	54.8 µF
Q-V droop coefficient	0.08
P-F droop coefficient	0.01
kp & ki of the current controller	kp = 0.005 , ki = 1
kp & ki of DC-link voltage control	kp = 0.15 , ki = 80

5.3 The first scenario: Simulation results without using the proposed control strategy

We implement a 50 kVA of three-phase grid inverter using the grid connection in this scenario. The PV source of the inverter have 800 DC voltage through an MPPT control, and the vector-oriented control with the PWM and DC-link voltage control can be used to govern the output of the inverter. First, a DC reference voltage is applied to get the maximum output power generated from the PV system, which is connected to PWM through a PI controller. Moreover, the LCL filter connects the inverter with the grid to remove the current ripples from PWM.

50 Hz & 10 kHz is the frequency and switching frequency, respectively, taken as the inverter's AC frequency. RL load type will be used because most of the loads in the network are of this type. The inverter will deliver all active power generated from the PV to the grid, and this thesis will study the effects on the voltage and frequency with any disturbance. The structure of the system for the first scenario is shown in figure A.21.

The objective of studying this case is to look at the grid-connected inverter dynamics and then to see where we can make the improvements in the network. The output DC voltage of the PV is 406 V (14*29), and through a boost converter will be hold as a constant 800 VDC as the input voltage to the inverter.

Figure A.22, shows the response of power during the normal conditions when the solar radiation varies from (0 to 1000) W/m^2 then from (1000 to 0) W/m^2 in clear sky day with load power equal to 120 kW and 37.5 kVAr.

In figure A.23 , we can observe that the voltage at load bus was varied from (201 to 204.7) V and this voltage is a low voltage. As a result, we can see in figure A.22(a) that the load power was varied between (100 to 103.7) kW, (31.2 to 32.2) kVAr, and the inverter power was varied between (0 to 50) kW as shown in figure A.22(c) and there is a high loss in active power at load bus.

Many disturbances can happen in the network, such as a sudden change in load, sudden change in solar radiation, unstable voltage source. However, the worst cases it is when:

a- The solar radiation is maximum and the load power is minimum.

b− The solar radiation is minimum and the load power is maximum.

5.3.1 High solar radiation with low load power

Firstly, when the solar radiation and load power are both low, the voltage (V1) is 212 V, as shown in figure A.24. secondly, when the solar radiation is high (1000 W/m^2) and the load is minimum and equal to (20 kW,7.5 kVAr), the voltage (V2) at load bus will be increased to 229.8 V as shown in figure A.24, and this increasing back to the power that generated from PV is more significant than the load power. As shown in figure A.25, this case creates a reverse power flow in the grid, which is a phenomenon which makes the system unstable and causes many problems like overvoltage in the feeders, rising fault current, and inappropriate use of the protective device [62].

5.3.2 Low solar radiation and high load power

When the solar radiation is low, like when it is 200 W/m^2, the expected power generated from the PV system (Ppv) is 10 kW, and after we ran the simulation, we observed that the load voltage was 202.4V, as shown in figure A.26. inverter power, active and reactive load power were 9 kW,100 kW,30 kVAr, respectively, as shown in figure 5.1, and these values are low and effects the operation and stability of the grid.

Figure 5.1

Grid, Inverter, Load active (kW) and reactive (kVAr) power with low solar radiation and low load power.

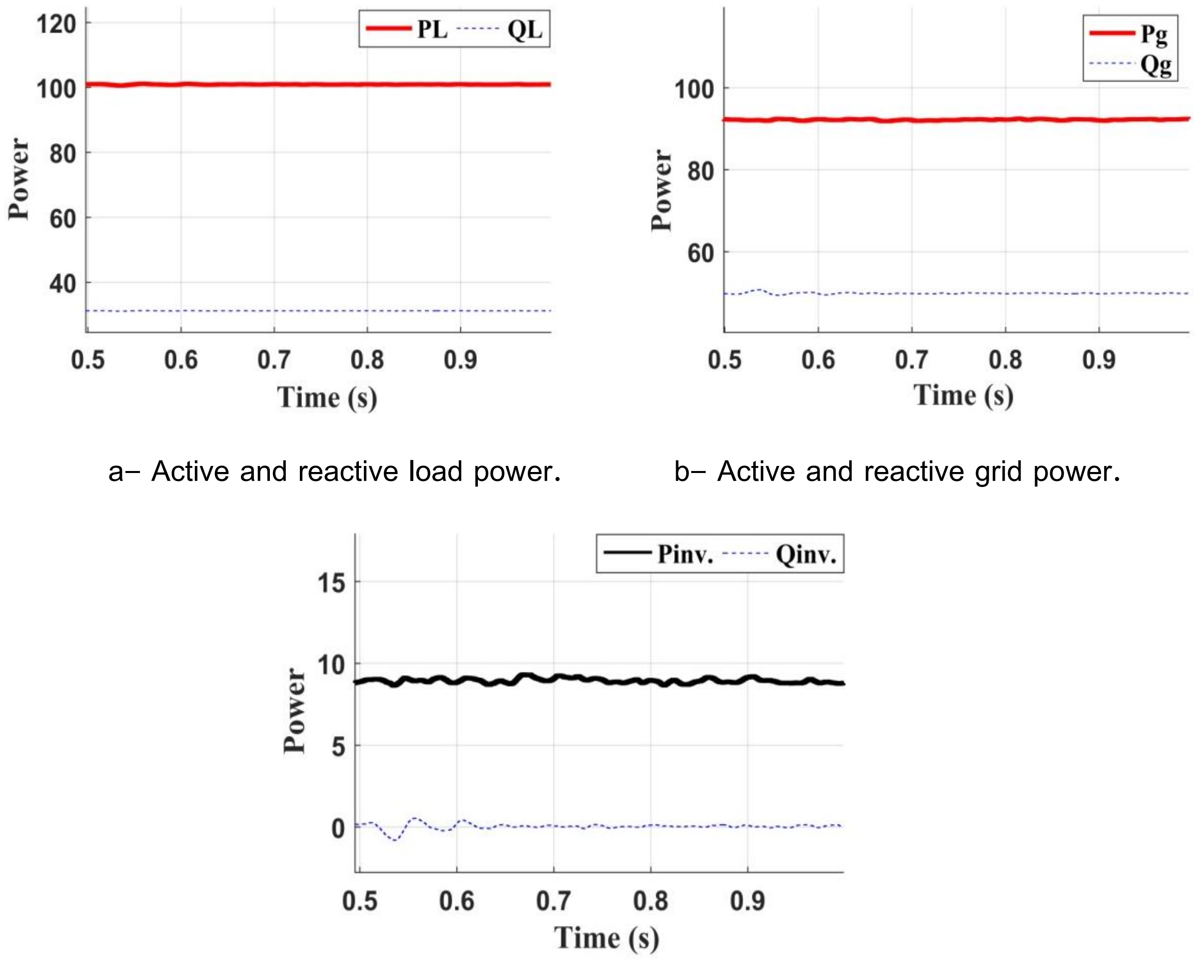

a– Active and reactive load power.

b– Active and reactive grid power.

c– Inverter output

5.4 The second scenario: Simulation results with using the proposed control strategy for voltage improvements

In this scenario, we implement the VSG with PRC control to reserve a specific part of the power for controlling the output power of the PV system, and control the output voltage at load bus according to the state of the grid.

5.4.1 Low solar radiation and high load power

The system response of the proposed control strategy with low active power generated from PV and high load power equal to 120 kW, 37.5 kVAr is shown in figure 5.2, and the load voltage improvement in figure A.27.

Figure 5.2

Grid, Inverter, Load active (kW) and reactive (kVAr) power with low solar radiation and high load power.

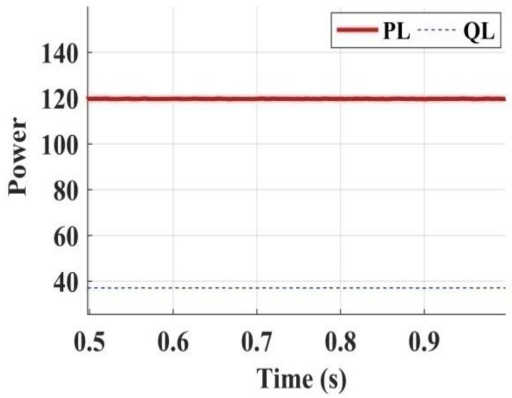

a– Active and reactive load power.

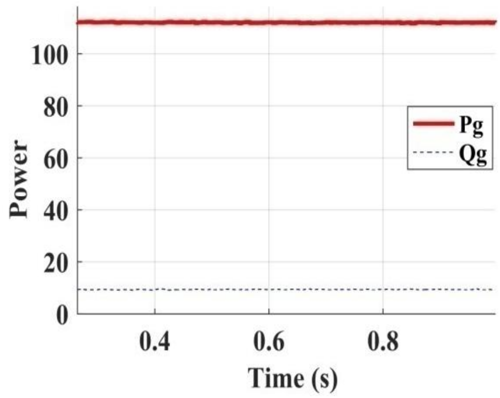

b– Active and reactive grid power.

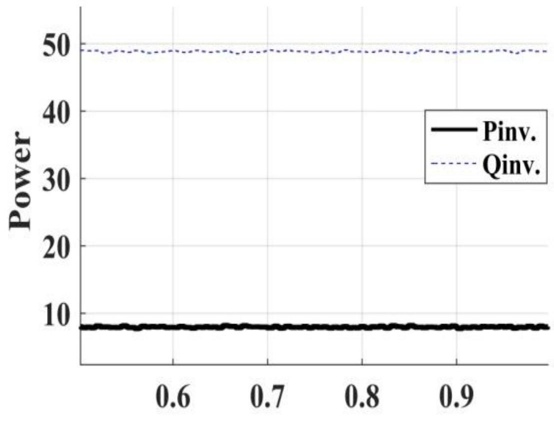

c– Inverter output power.

5.4.2 High solar radiation with low load power

The system response and voltage improvements when we use the proposed control strategy with high active power generated from the PV and low load power equal to 20 kW, 7.5 kVAr is as shown in figures A.28 and 5.3.

Figure 5.3

Grid, Inverter, Load active (kW) and reactive (kVAr) power with high solar radiation and low load power.

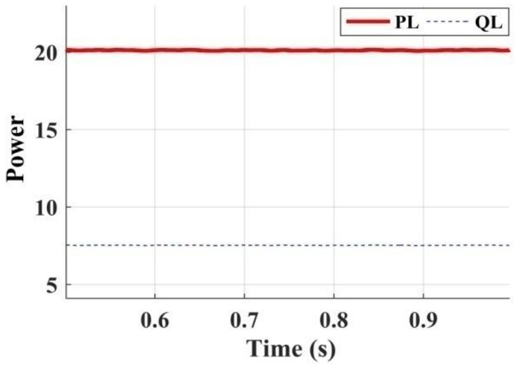

a– Active and reactive load power.

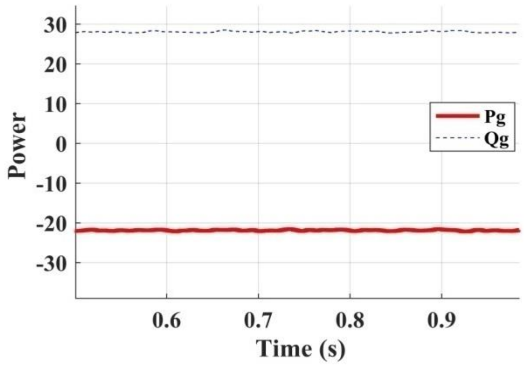

b– Active and reactive grid power.

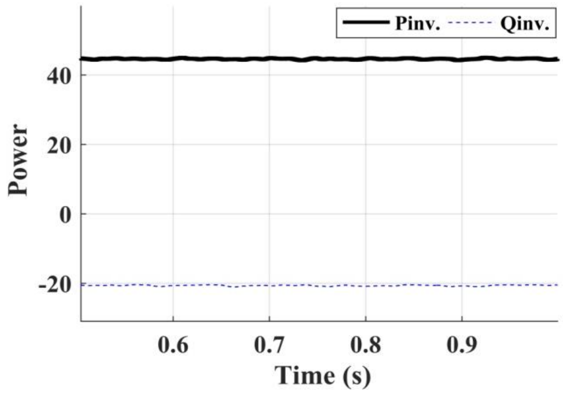

c– Inverter output power.

5.5 The third scenario: Simulation results with using the proposed control strategy for frequency improvements

In this scenario, we implement the VSG with PRC control to reserve a specific part of the power for controlling the output power of the PV system and regulate the system frequency according to the state of the grid.

5.5.1 High level of solar radiation with system frequency rise

After the simulation, the results of increasing system frequency from 50 Hz to 50.4 Hz are shown in figures 5.4.a and 5.4.b.

Figure 5.4.a

Reserve and inverter active power (kW).

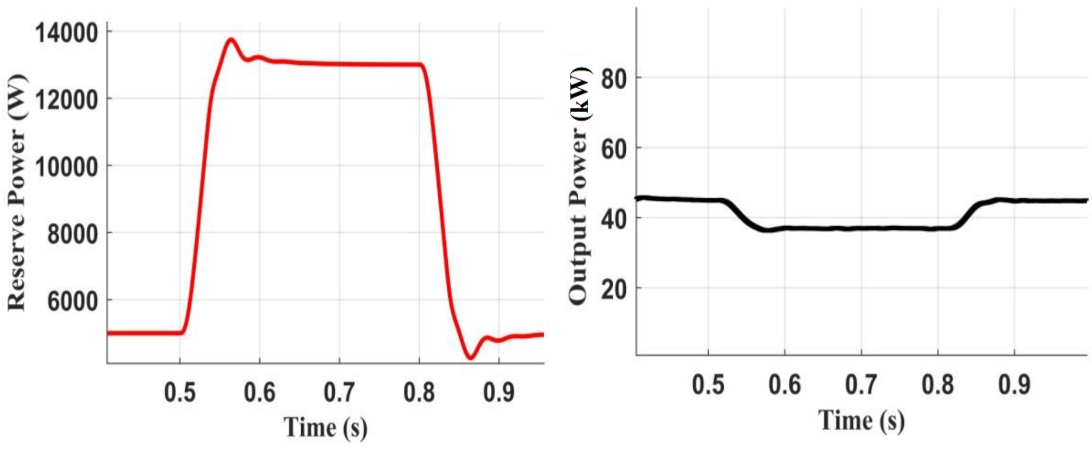

a– Reserve power (kW). b– Inverter output with PRC control.

Figure 5.4.b

System response with frequency rise.

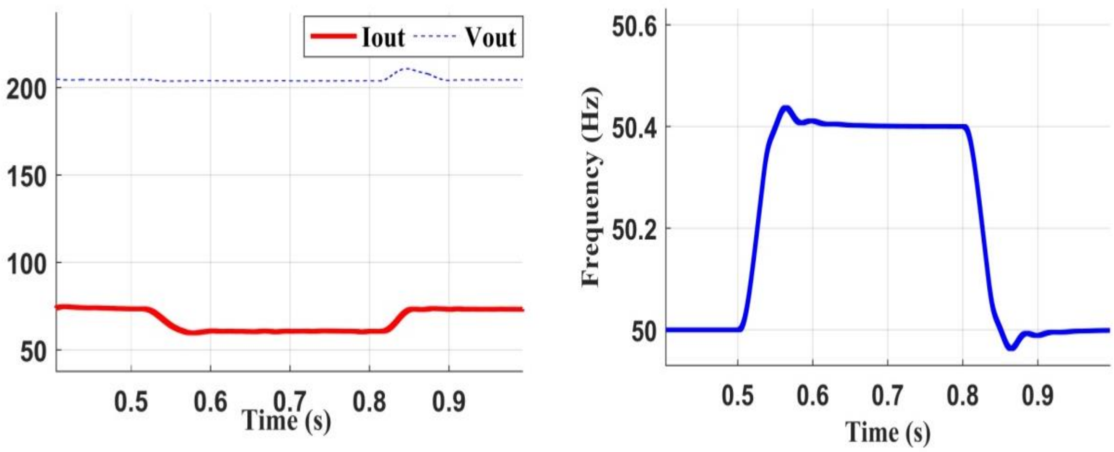

a– Output load voltage (V) and current (A). b– Grid frequency.

5.5.2 System frequency drops significantly or decrease in a small range

After the simulation, the results of decreasing system frequency in a small range from 50 Hz to 49.85 Hz are shown in Figures 5.5.a and 5.5.b.

Figure 5.5.a

Reserve and inverter active power (kW).

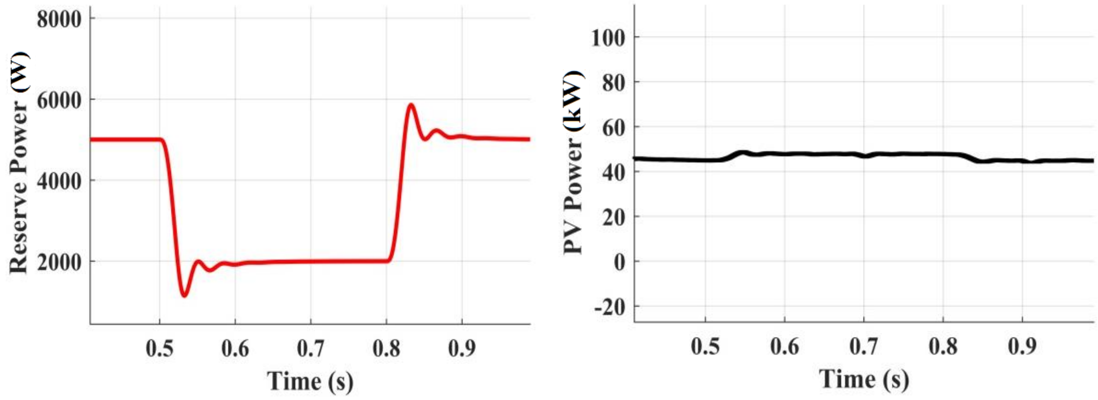

a– Reserve power (kW). b– Inverter output with PRC control.

Figure 5.5.b

System response with small frequency drop.

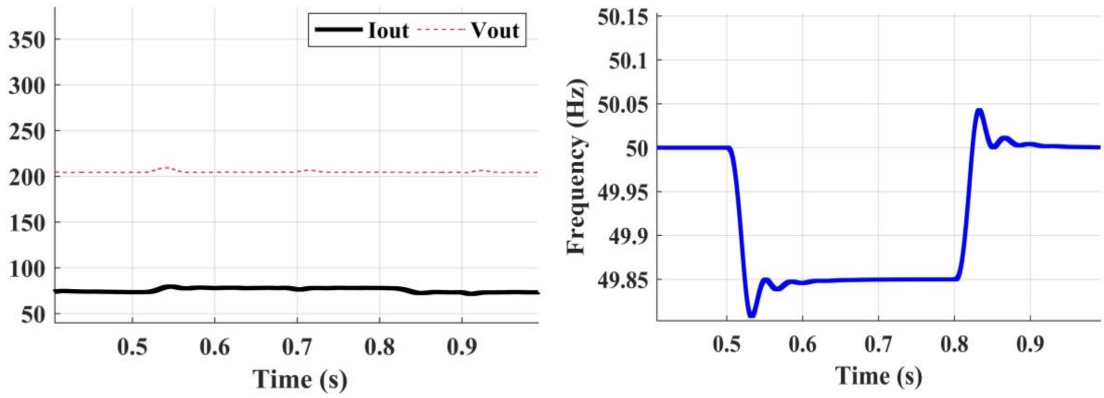

a– Output voltage and current. b– Grid frequency.

However, when the frequency decreased in a high range from 50 Hz to 49.6, the results are as seen in Figures 5.6.a and 5.6.b.

Figure 5.6.a

Reserve, inverter active power (kW).

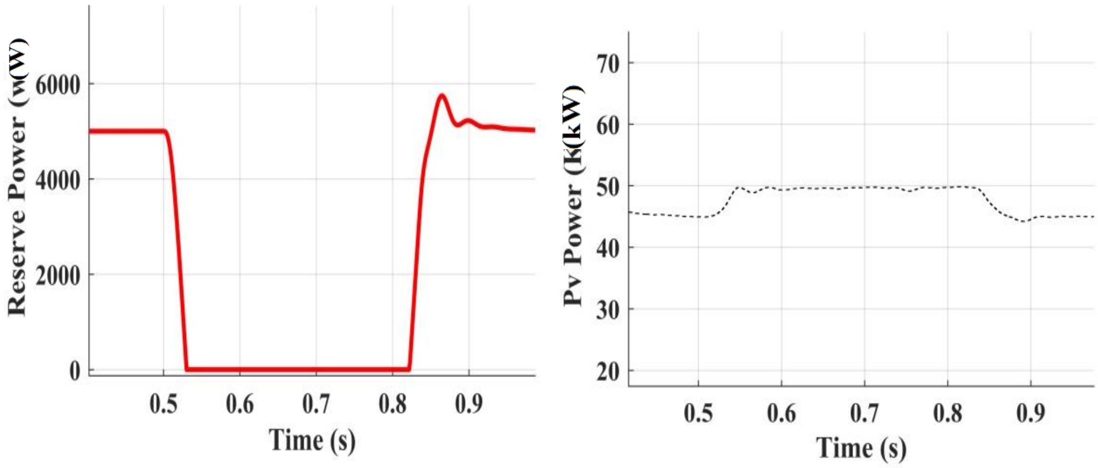

a– Reserve power (kW). b– Inverter output with PRC control.

Figure 5.6.b

System response with high-frequency drop.

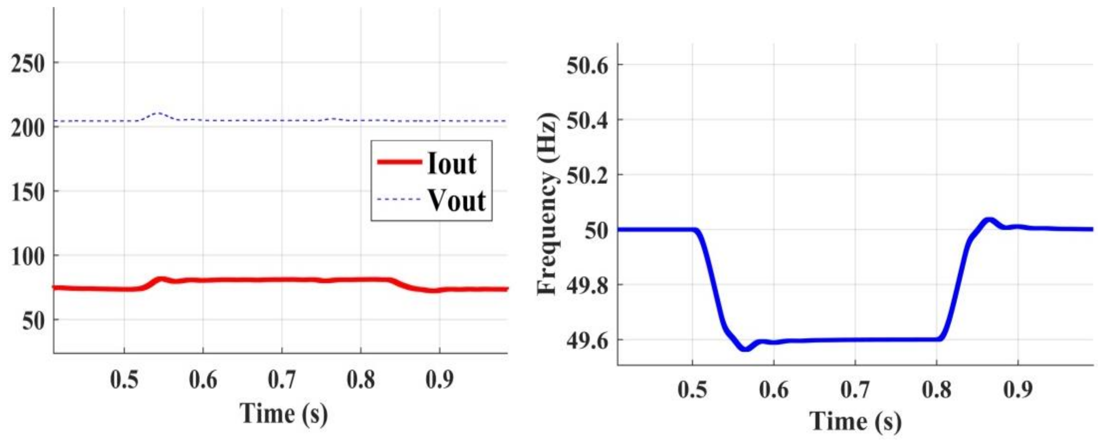

a– Output voltage and current. b– Grid frequency.

5.6 The fourth scenario: Simulation results with using the proposed control strategy for frequency and voltage improvements

In this scenario, we implement the VSG with PRC control to reserve a specific part of the power for controlling the output power of the PV system, control the output voltage at the load bus and regulate the system frequency according to the state of the grid.

When the solar radiation is 600 W/m^2 and the load power is high (120 kW, 37.5 kVAr), the inverter output power is shown in figure A.29.

When there is a system frequency rise from 50 Hz to 50.2 Hz, the reserve power increases, as shown in figure A.30.

The load voltage, in this case, increased from 204V to 219V, as shown in figure A.31.

5.7 Scenarios discussions

After run the simulation and presented the results in the previous chapter, these results will be discussed and compared in this chapter.

In figures A.22 and A.23 can be seen that this grid during the normal conditions has a lower power and voltage that may affects the operation of electrical appliances and the voltage/frequency system stability. So, there is a need to use the appropriate control to improve the voltage profile and solve this problem, and it is the reason to use the proposed control strategy.

In the case of low solar radiation with high load power, figures 5.2 and A.27 presented that the voltage at load bus and grid reached to 220 V, and the active PV power was 8 kW when we used the proposed control strategy that responsible for introducing a certain reactive power from the PV system (49 kVAr) instead of absorbing all reactive power that needed from the source. In addition, we can observe that there is an improvement in voltage when we compare these results with the results in figures 5.1 and A.26.

The next table shows the improvements that happened in this case:

Table 5. 2:

Grid improvement with low solar radiation.

	MPPT inverter	VSG-PRC inverter
load voltage	202.4 V	220 V
Active and reactive power of the inverter	8.8 kW, 0	7.9 kW, 48.8 kVAr
Active and reactive power of the grid	92.35 kW, 49.82 kVAr	112 kW, 9.2 kVAr
Active and reactive load power	100.9 kW, 31 kVAr	119.6 kW, 37 kVAr

From table 5.1, we can observe that there is an improvement in voltage and load power, which make the system more stable. Also, reducing the reactive power absorbed from the grid reduces the grid losses and decreases the effects of high penetration levels of PV systems in the network.

When the solar radiation and load power both are low, we can see in figure A.24 that the voltage was 212 V. Then, when the power generated from the PV system becomes bigger and bigger than the active load power, the load voltage increases to 230 V because there is a large power reverse from the PV system towards the grid (about 27 kW), as shown in figure A.25. This increase in voltage and power reverse affects the system stability. So, we used the proposed control strategy to reduce the effect of reverse power in the grid by making the inverter acting as a synchronous generator to absorb an amount of reactive power from the grid (20 kVAr) to regulate the load voltage to be 220 V depending on equations 4.1, 4.2 and 4.4. According to the de-load control, reducing the output of the PV system reduces the effect of reverse power. These improvements when using the VSG with the PRC controller makes the system more stable, as shown in figures A.28 and 6.3.

In the case of system frequency rise, when the system has a surplus power at a certain moment, this results in a change of frequency in the grid. It varies from 50 to 50.4 Hz, and then it returns back to the normal condition after the problem is cleared. Figure 5.4.b presents the variation of system frequency during and after the surplus power problem in the system.

During the regular operation at rated frequency, the reserve value will be 10%Pn according to the regulations mentioned before in chapter six, and it is equal to 5 kW. Then when the frequency increase, the reserve power is increased to be 13 kW (26% Pmpp), and the output power of the PV system will be reduced from 45 kW to 37 kW according to the relation between frequency and reserve power described in equation 4.5 in chapter 6 as shown in figure 5.4.a. In figure 5.4.b, we can see that the output voltage is still constant, and the current of the inverter decreases when the inverter power decreased. All of these values are consistent with equations 4.5 and 4.8. By reserving a specific part of PV power, the process of system frequency response effectively ensures power system stability.

In case of system frequency drops significantly or in a small range, the amount of reserve power during regular operation and the simulation parameters are just like above

(10%Pmpp). The frequency decreases in small and high ranges when a generator fails or a sudden cut of a large load happened.

Firstly, drops in a small range, such as when it reduces from 50 to 49.85 Hz for a particular time, then after the fault is clear, it returns to the rated value (50 Hz), as seen in figure 5.5.b. Then, in figure 5.5.a, the reserve power will decrease from 5 kW to 2 kW, and the power generated from the PV will increase in a specific value (3 kW) to support the system according to equation 4.5.

The reserve ratio will decrease from (10% to 4%) Pmpp according to equations 4.7 and 4.8. Also, in figure 5.5.b, the output voltage and current of the three-phase inverter are presented.

Secondly, the frequency drops in a high range, from 50 to 49.6 Hz. Then after the fault is clear, it backs to the normal operation, as shown in figure 5.6.b.

According to equations 4.8 and 4.9, there will be a limit to the FR because there is a limitation in reserve power in PV systems. When the frequency decrease more than 0.33 Hz, the PV inverter will operate like in MPPT mode to introduce all active power generated from the PV system. From figure 5.6.a, we can see that the reserve power decreased from 5 kW to zero, and the power generated from PV is maximum, equal to 50 kW for participating in the grid.

Those values presented in figures 5.4 to 5.6 are consistent with the previous equations mentioned before. By releasing/decreasing a part or all of the reserve power from PV, we can see that participating in FR of the grid was effective without using the energy storage devices. Additionally, the period of support active power has extended.

In this case, when the solar radiation is 600 W/m^2, and there is a variation in the frequency by +0.2 Hz from the nominal, we can see that the voltage was 204V, as shown in figure A.31. The proposed control strategy improved the voltage by 14V to be 218 V by introducing the required reactive power to improve the voltage and improved the frequency to be 50 Hz by reducing a certain amount of the active output power of the PV system, as shown in figure A.30. These improvements in system frequency and voltage make the system more stable.

5.8 Conclusion

Some distributed generation that uses renewable energy sources is unsuitable for direct grid integration. So, the power electronic inverters must be used as a link between the distributed generation and the grid. Still, the lack of inertia in these inverters causes problems in grid stability.

The grid inverters cannot minimize these problems. However, the traditional synchronous generator can solve these problems, so the VSG concept was born with the grid inverter to emulate the behavior of SGs.

In traditional VSG control, we need energy storage systems which are highly expensive and giving rise to the cost of PV systems. In this thesis, we proposed a new method of VSG control which is the new VSG control without using the energy storage systems.

Activating the DC/DC converter allows the PV system's reserve power to be realized. The output power can be controlled to allow the solar PV system to have individual frequency support and perform power conversion. A power electronics inverter is used, as well as the reactive power regulations.

The grid in this thesis was weak. Only one inverter (50 kVAr) was used, and its effects on the grid were that the voltage decreased by approximately 15 V in most cases. Therefore, when the proposed control strategy was used, the voltage was improved by (10-20) V to be 220 V, to make the system more stable.

In the smart grid and by using the data centers, the cases when the system frequency can rise or fall can be predicted when these cases will occur. So, based on the data and with using the proposed control, the inverter will reduce the output power of the PV system by a certain amount and use this power as a reserve power to support the grid. As a result, the frequency in this thesis is improved by (±0.4) Hz. Noticing that one inverter was used in this thesis, but there is more than one inverter in the grid in the real case. Therefore, the number of effects and improvements is more significant than using one inverter.

The next conclusions obtained from the analysis and simulation results:

1- Reduce the high effects of the large penetration level of PV distributed generations.
2- Voltage and frequency profile improvement.

3- PRC technique in this thesis can operate in both modes: MPPT and PRC based on the actual grid requirements and there is no need to change the control method to switch between them.
4- The operating point of voltage in the proposed method is always on the right side of the maximum power point voltage method to operate the inverter safely and effectively.
5- There is no need for a complicated PV array modeling or estimation algorithm.
6- Economic. No need for the energy storage systems for participating power in the frequency response of the power system.

The disadvantage of this method it has a limitation on the reserve power but on the other hand, it offers a longer duration of power support when compared with battery storage.

5.9 Future work

This section discusses an expansion of this study in six areas to fulfill the thesis requirements.

1- Verifying simulation results practically in the laboratory.
2- Making this control on multi-inverters connected to the grid.
3- PI controller gains in the current simulation have been chosen by trial and error method and this could be the source of the system oscillation. As a result, we need to create mathematical equations to calculate these gains accurately.
4- This study focused on the grid-connected mode that will need to be expanded to include island mode.
5- Propose a solution to prevent the limitation on reserve power.

List of Abbreviations

Abbreviation	Meaning
AC	Alternative Current
ALFC	Automatic Load Frequency Control
AVR	Automatic Voltage Regulator
DC	Direct Current
EMF	Electro-Motive Force in the stator
ESSs	Energy Storage Systems
FR	Frequency Response
IEPE	Institute of Electrical Power Engineering
ISE	INGENIA Solar Energy
KHI	Kawasaki Heavy Industries
MPP	the Maximum Power Point
MPPE	Maximum Power Point Estimation
MPPT	the Maximum Power Point Tracker
N	Neutral line
PH	Phase line
PLL	Phase Locked Loop
PRC	Power Reserve Control
PVs	photovoltaic systems
PWM	Pulse Width Modulation
REs	Renewable Energy Systems
RES	Renewable Energy Sources
SC	Series Compensator
SG	Synchronous Generator
SMs	Synchronous Machines
SOC	State Of Charge
SSSC	Static Synchronous Series Compensator
STATCOM	Static Compensator
THD	Total Harmonic Distortion
VCO	Voltage-Controlled
VOC	Vector Oriented Control
VSA	Virtual Synchronous Algorithm
VSG	Virtual Synchronous Generator
VISMA	Virtual Synchronous Machine research group
VSYNC	Virtual Synchronous group
VSG_ PRC	Virtual Synchronous Generator with Power Reserve Control

References

1. Putrus, G. and E. Bentley, Integration of distributed renewable energy systems into the smart grid. Electric Renewable Energy Systems, 2016: p. 487-518.

2. Uzum, B., et al., Rooftop Solar PV Penetration Impacts on Distribution Network and Further Growth Factors—A Comprehensive Review. Electronics, 2021. 10(1): p. 55.

3. Union, E., Directive 2009/28/EC of the European Parliament and of the Council of 23 April 2009 on the promotion of the use of energy from renewable sources and amending and subsequently repealing Directives 2001/77/EC and 2003/30/EC. Official Journal of the European Union, 2009. 5: p. 2009.

4. Ogimoto, K., et al., A good fit: Japan's solar power program and prospects for the new power system. IEEE Power and Energy Magazine, 2013. 11(2): p. 65-74.

5. Bevrani, H., T. Ise, and Y. Miura, Virtual synchronous generators: A survey and new perspectives. International Journal of Electrical Power & Energy Systems, 2014. 54: p. 244-254.

6. Koyanagi, K., et al. A smart photovoltaic generation system integrated with lithium-ion capacitor storage. in 2011 46th International Universities' Power Engineering Conference (UPEC). 2011. VDE.

7. Kundur, P., et al., Definition and classification of power system stability IEEE/CIGRE joint task force on stability terms and definitions. IEEE transactions on Power Systems, 2004. 19(3): p. 1387-1401.

8. Mohammed, O., et al., Virtual synchronous generator: an overview. Nigerian Journal of Technology, 2019. 38(1): p. 153-164.

9. Slootweg, J. and W. Kling. Impacts of distributed generation on power system transient stability. in IEEE Power Engineering Society Summer Meeting. 2002. IEEE.

10. Driesen, J. and K. Visscher. Virtual synchronous generators. in 2008 IEEE power and energy society general meeting-conversion and delivery of electrical energy in the 21st century. 2008. IEEE.

11. Sakimoto, K., Y. Miura, and T. Ise. Stabilization of a power system with a distributed generator by a virtual synchronous generator function. in 8th International Conference on Power Electronics-ECCE Asia. 2011. IEEE.

12. Visscher, K. and S.W.H. De Haan. Virtual synchronous machines (VSG's) for frequency stabilisation in future grids with a significant share of decentralized generation. in CIRED Seminar 2008: SmartGrids for Distribution. 2008. IET.

13. Bevrani, H. and T. Hiyama, Intelligent automatic generation control. 2011: CRC press New York.

14. Liu, H., et al. Impact of high penetration of solar photovoltaic generation on power system small signal stability. in 2010 international conference on power system technology. 2010. IEEE.

15. D'Arco, S., J.A. Suul, and O.B. Fosso, A Virtual Synchronous Machine implementation for distributed control of power converters in SmartGrids. Electric Power Systems Research, 2015. 122: p. 180-197.

16. Saborio Romano, O., Small-signal modelling and stability analysis of a traditional generation unit and a virtual synchronous machine in grid-connected operation. 2015, NTNU.

17. Kundur, P., Power system stability and control. 7 McGraw-Hill. Inc., New York, 1994.

18. Kothari, D.P. and I. Nagrath, Modern power system analysis. 2003: Tata McGraw-Hill Education.

19. Feng, C., et al., Advanced machine learning applications to modern power systems, in New Technologies for Power System Operation and Analysis. 2021, Elsevier. p. 209-257.

20. Machowski, J., et al., Power system dynamics: stability and control. 2020: John Wiley & Sons.

21. Donsion, M.P., J. Guemes, and J. Rodriguez. Power Quality. Benefits of Utilizing FACTS Devices in Electrical Power Systems. in 2007 7th International Symposium on Electromagnetic Compatibility and Electromagnetic Ecology. 2007. IEEE.

22. Meng, X. and Z. Pian, Intelligent coordinated control of complex uncertain systems for power distribution and network reliability. 2015: Elsevier.

23. Tang, Y., Voltage stability analysis of power system. 2021: Springer.

24. Qu, J. and J. Guo, Statistics and analysis of faults in main domestic power systems from 1996 to 2000. Power system technology, 2004. 28(21): p. 60-63.

25. LIU, Y.-q. and K. Xie, Analysis on blackout of interconnected North America power grid occurred on AUG. 14, 2003 from the viewpoint of power system dispatching [J]. Power System Technology, 2004. 8.

26. Srivastava, P. and R. Pardhi, A review on power system stability and applications of fact devices. Int. J. Eng. Res. Appl., 2013. 3(2): p. 879-883.

27. Abdulraheem, B.S. and C.K. Gan, Power system frequency stability and control: Survey. International Journal of Applied Engineering Research, 2016. 11(8): p. 5688-5695.

28. Standard, B., Voltage characteristics of electricity supplied by public distribution networks. BS EN, 2007.

29. Loix, T., et al. Layout and performance of the power electronic converter platform for the VSYNC project. in 2009 IEEE Bucharest PowerTech. 2009. IEEE.

30. Chen, Y., et al., Dynamic properties of the virtual synchronous machine (VISMA). Proc. Icrepq, 2011. 11: p. 755-759.

31. Chen, Y., et al., Comparison of methods for implementing virtual synchronous machine on inverters. Renewable energy & power quality journal, 2012: p. 734-739.

32. Chen, Y., et al. Improving the grid power quality using virtual synchronous machines. in 2011 international conference on power engineering, energy and electrical drives. 2011. IEEE.

33. Hesse, R., D. Turschner, and H.-P. Beck. Micro grid stabilization using the virtual synchronous machine (VISMA). in Proceedings of the International Conference on Renewable Energies and Power Quality (ICREPQ'09), Valencia, Spain. 2009.

34. Alipoor, J., Y. Miura, and T. Ise, Power system stabilization using virtual synchronous generator with alternating moment of inertia. IEEE journal of Emerging and selected topics in power electronics, 2014. 3(2): p. 451-458.

35. Sakimoto, K., Y. Miura, and T. Ise, Stabilization of a power system including inverter type distributed generators by the virtual synchronous generator. IEEJ Transactions on Power and Energy, 2012. 132(4): p. 341-349.

36. Shintai, T., Y. Miura, and T. Ise. Reactive power control for load sharing with virtual synchronous generator control. in Proceedings of The 7th International Power Electronics and Motion Control Conference. 2012. IEEE.

37. ALIPOOR, J., Y. MIURA, and T. ISE, Evaluation of virtual synchronous generator (VSG) operation under different voltage sag conditions. 電気学会研究会資料. PE, 電力技術研究会, 2012. 2012(52): p. 41-46.

38. Hirase, Y., et al., A grid-connected inverter with virtual synchronous generator model of algebraic type. Electrical Engineering in Japan, 2013. 184(4): p. 10-21.

39. Bao, G., et al., A novel photovoltaic virtual synchronous generator control technology without energy storage systems. Energies, 2019. 12(12): p. 2240.

40. Sood, V.K. and H. Abdelgawad, Power converter solutions and controls for green energy. Distributed Energy Resources in Microgrids, 2019: p. 357-387.

41. Dileep, D.K. and K. Bharath. A brief study of solar home inverters. in 2018 International Conference on Control, Power, Communication and Computing Technologies (ICCPCCT). 2018. IEEE.

42. Gazoli, J.R., M.G. Villalva, and E. Ruppert, Micro-inverter for integrated grid-tie photovoltaic module using resonant controller. International Transactions on Electrical Energy Systems, 2014. 24(5): p. 713-722.

43. Phap, V.M., Le Thi Thuy Hang.“Comparison of Central Inverter and String Inverter for Solar Power Plant: Case Study in Vietnam”. Journal of Nuclear Engineering & Technology, 2019. 9(3): p. 11-23p.

44. Khallaf, M., Enhanced MPPT controllers for smart grid applications. 2019: Rochester Institute of Technology.

45. Hlaili, M. and H. Mechergui, Comparison of different MPPT algorithms with a proposed one using a power estimator for grid connected PV systems. International Journal of Photoenergy, 2016. 2016.

46. De Souza, K., M. De Castro, and F. Antunes. A DC/AC converter for single-phase grid-connected photovoltaic systems. in IEEE 2002 28th Annual Conference of the Industrial Electronics Society. IECON 02. 2002. IEEE.

47. Chung, S.-K., A phase tracking system for three phase utility interface inverters. IEEE Transactions on Power electronics, 2000. 15(3): p. 431-438.

48. Frenzel, L., Electronics Explained: Fundamentals for Engineers, Technicians, and Makers. 2017: Newnes.

49. Crecraft, D. and S. Gergely, Analog Electronics: circuits, systems and signal processing. 2002: Elsevier.

50. Blaabjerg, F., et al., Overview of control and grid synchronization for distributed power generation systems. IEEE Transactions on industrial electronics, 2006. 53(5): p. 1398-1409.

51. Crăciun, B.-I., et al., Frequency support functions in large PV power plants with active power reserves. IEEE Journal of Emerging and Selected Topics in Power Electronics, 2014. 2(4): p. 849-858.

52. Kazmierkowski, M.P. and L. Malesani, Current control techniques for three-phase voltage-source PWM converters: A survey. IEEE Transactions on industrial electronics, 1998. 45(5): p. 691-703.

53. Paspatis, A.G. and G.C. Konstantopoulos, Voltage support under grid faults with inherent current limitation for three-phase droop-controlled inverters. Energies, 2019. 12(6): p. 997.

54. Liu, B. and B.-M. Song. Modeling and analysis of an LCL filter for grid-connected inverters in wind power generation systems. in 2011 IEEE Power and Energy Society General Meeting. 2011. IEEE.

55. Kim, C.-K., et al., HVDC transmission: power conversion applications in power systems. 2009: John Wiley & Sons.

56. Zhong, C., et al., Virtual synchronous generator of PV generation without energy storage for frequency support in autonomous microgrid. International Journal of Electrical Power & Energy Systems, 2022. 134: p. 107343.

57. Zhang, X., et al., Coordinated control strategy for a PV-storage grid-connected system based on a virtual synchronous generator. Global Energy Interconnection, 2020. 3(1): p. 51-59.

58. Rehman, H.U., et al., An advanced virtual synchronous generator control technique for frequency regulation of grid-connected PV system. International Journal of Electrical Power & Energy Systems, 2021. 125: p. 106440.

59. Sangwongwanich, A., et al., Benchmarking of constant power generation strategies for single-phase grid-connected photovoltaic systems. IEEE Transactions on Industry Applications, 2017. 54(1): p. 447-457.

60. Tafti, H.D., et al., An adaptive control scheme for flexible power point tracking in photovoltaic systems. IEEE Transactions on Power Electronics, 2018. 34(6): p. 5451-5463.

61. Sangwongwanich, A., et al., Delta power control strategy for multistring grid-connected PV inverters. IEEE Transactions on Industry Applications, 2017. 53(4): p. 3862-3870.

62. Rahman, S., et al. Reverse power flow protection in grid connected PV systems. in SoutheastCon 2018. 2018. IEEE.

Appendix A

Figures of study

Figure A.1

Modern power system [19]

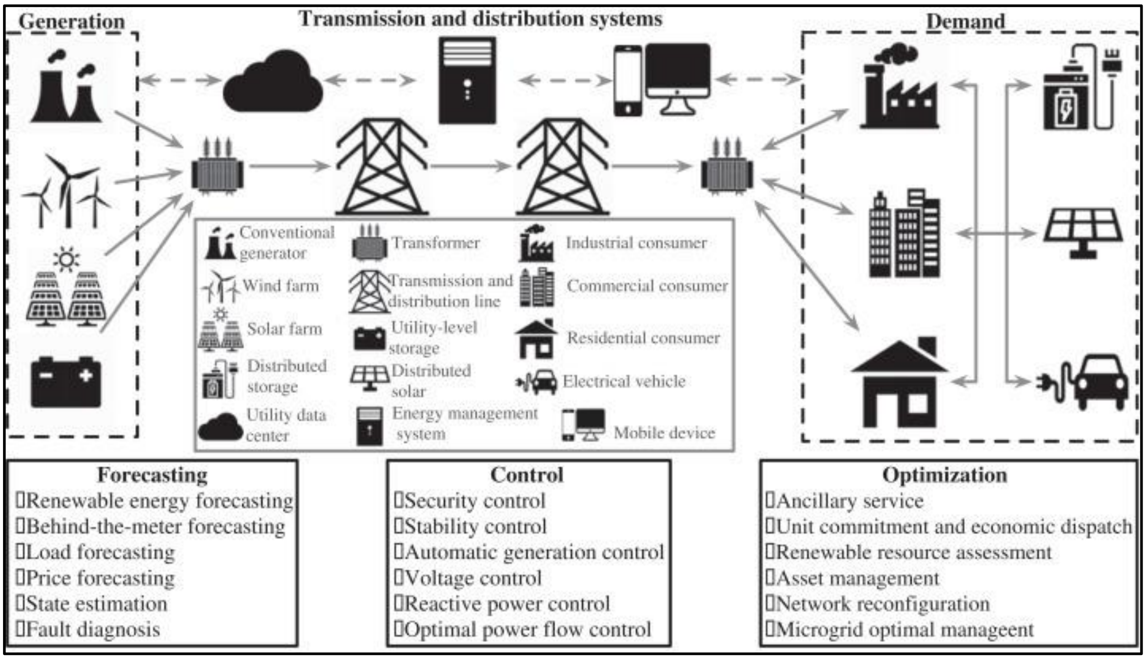

Figure A.2

Classifications of power system stability [7]

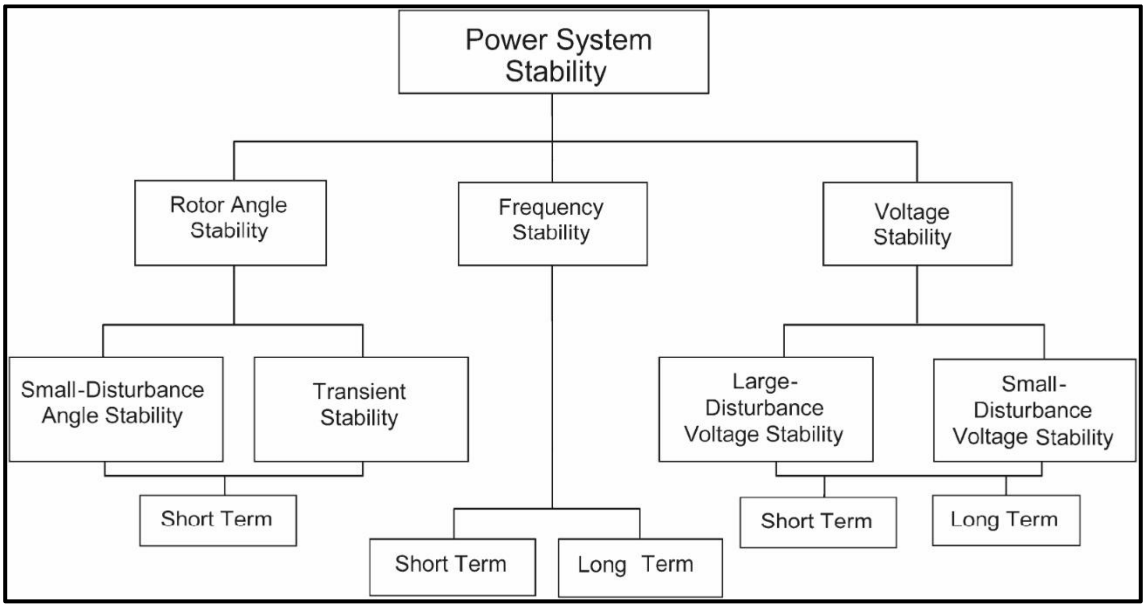

Figure A.3

VSG's main structure [11]

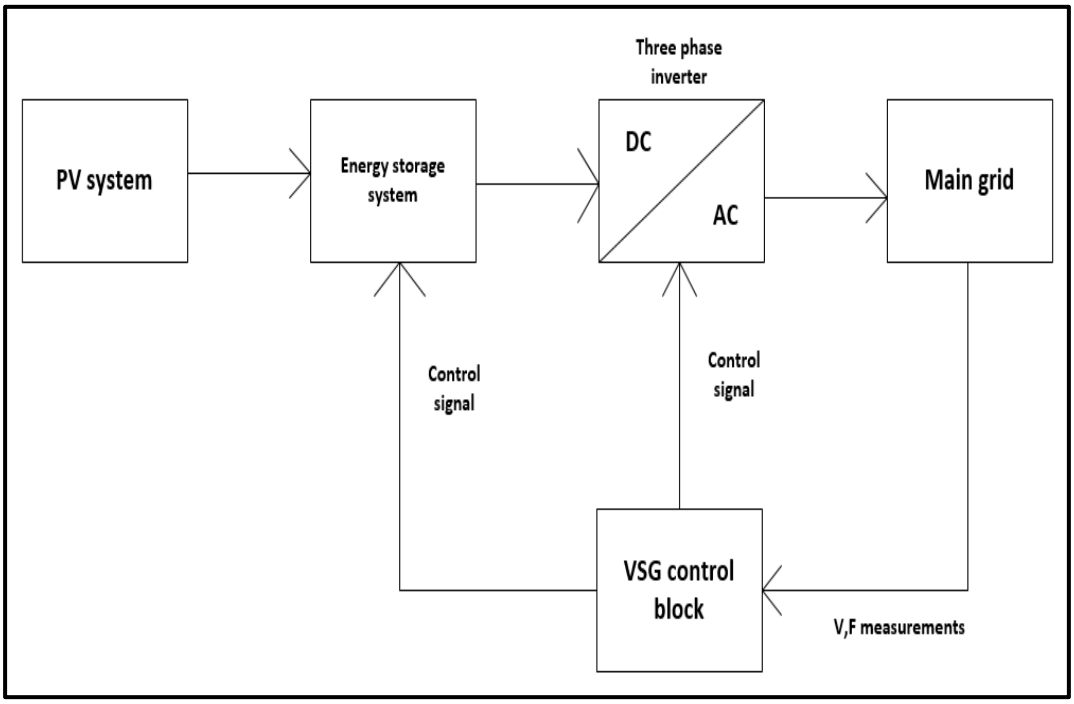

Figure A.4

The structure of VSG control according to ISE group [34].

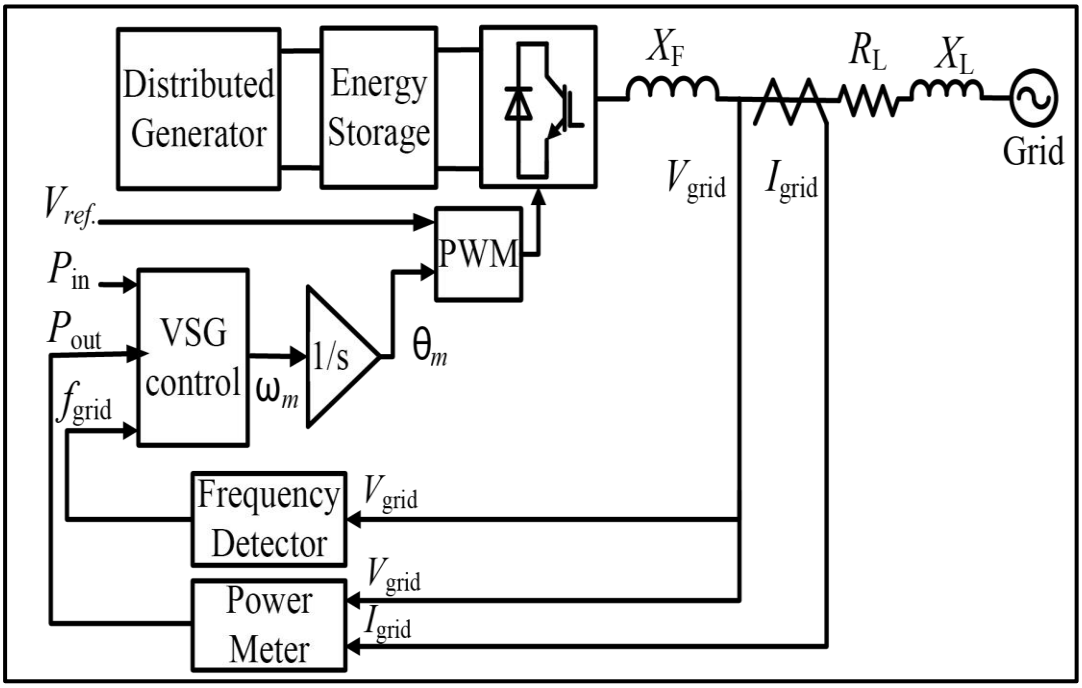

Figure A.5

Block diagram of VSG control according to KHI [38].

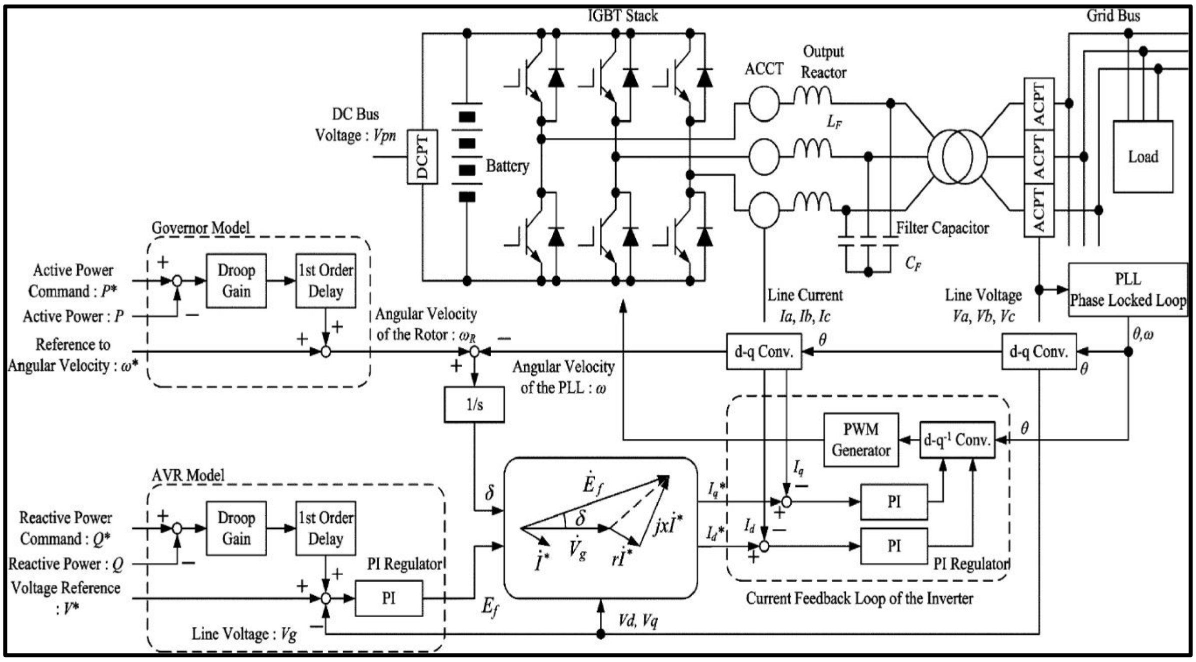

Figure A.6

Phasor-diagram of synchronous generator [38].

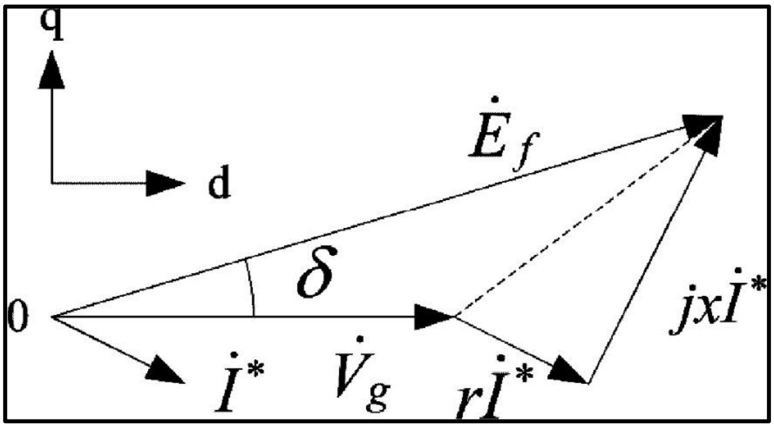

Figure A.7

The main structure of VSG control by the VSYNC research group [10].

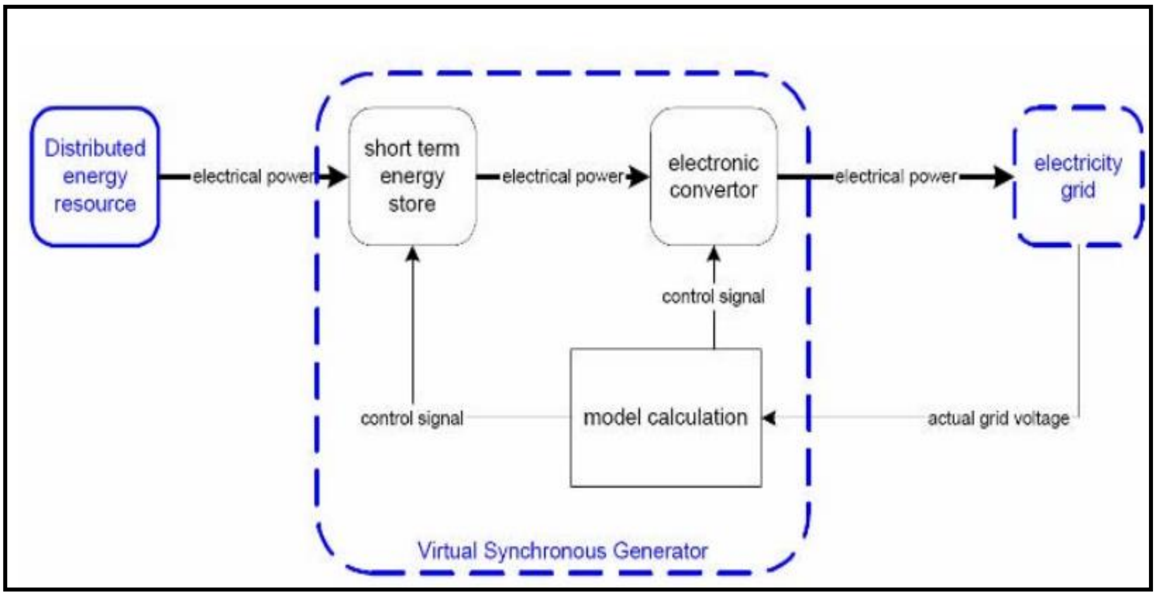

Figure A.8

The traditional control scheme of grid-connected inverter

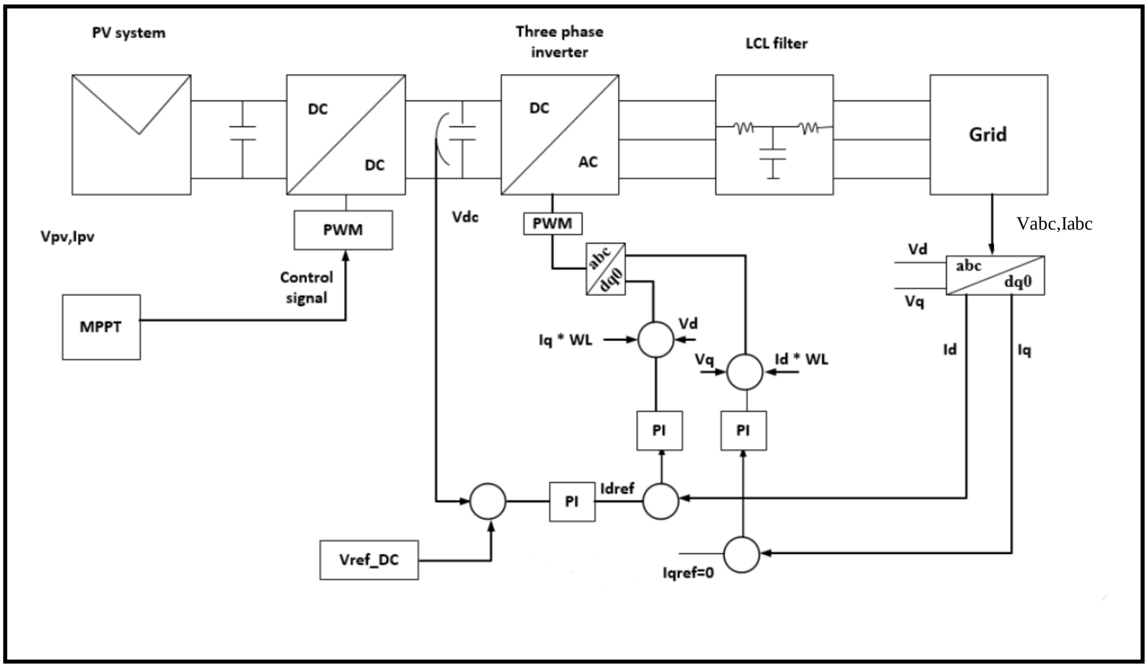

Figure A.9

The V-I characteristic curve [43].

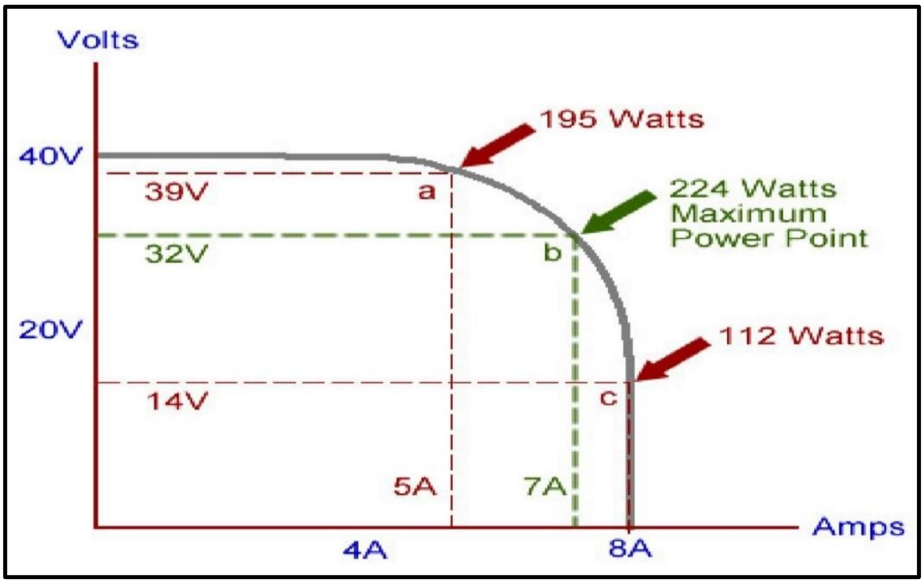

Figure A.10

The internal structure of PLL [49].

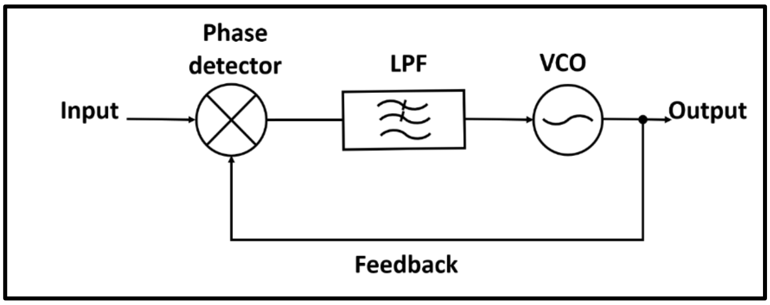

Figure A.11

The LCL filter circuit.

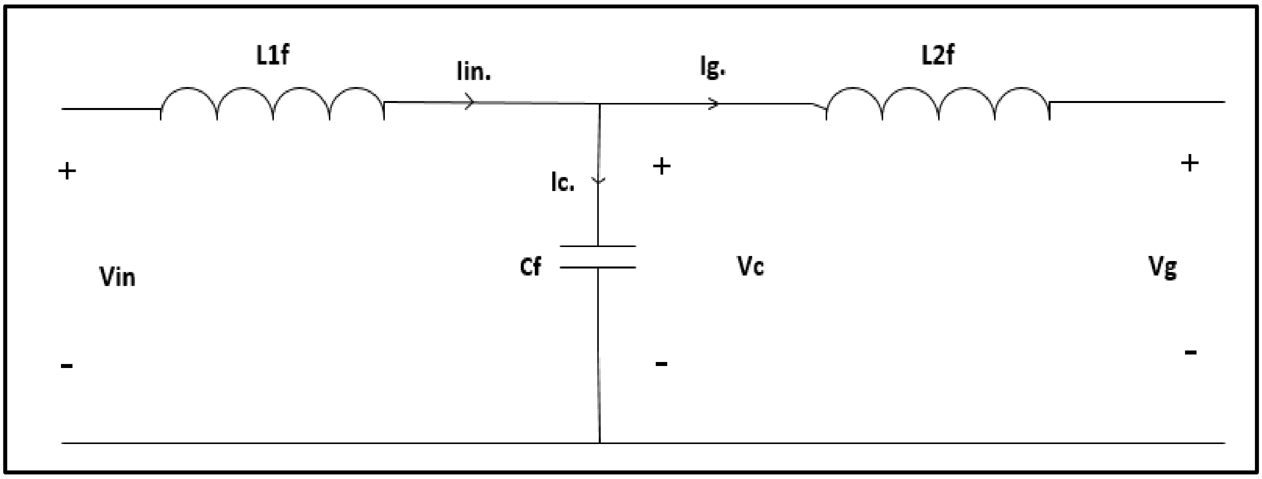

Figure A.12

The internal structure of the current control strategy.

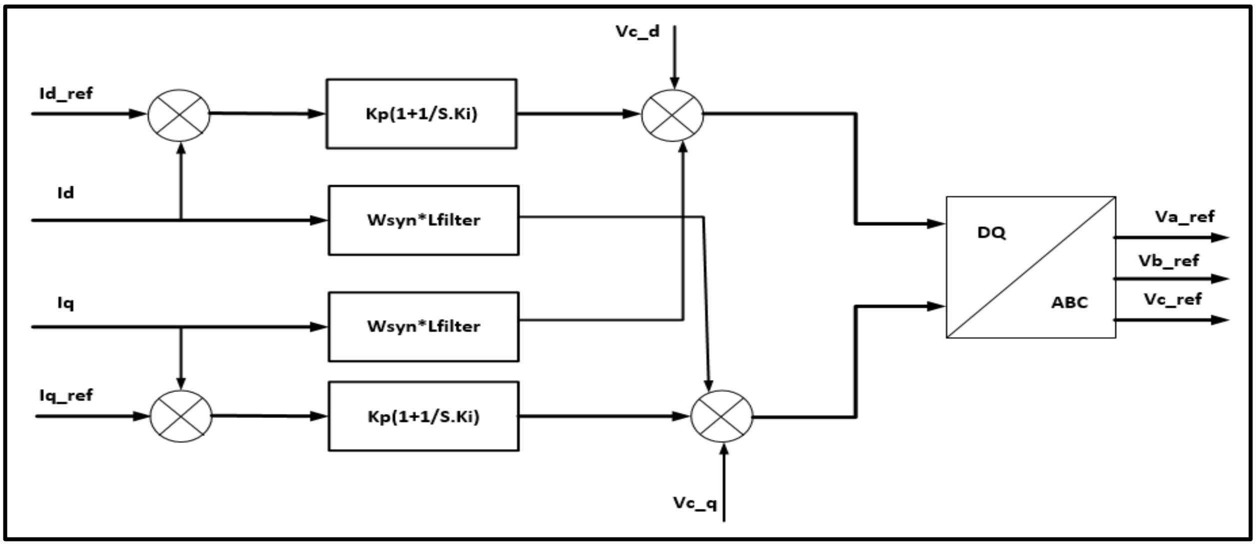

Figure A.13

The DC-link voltage control diagram.

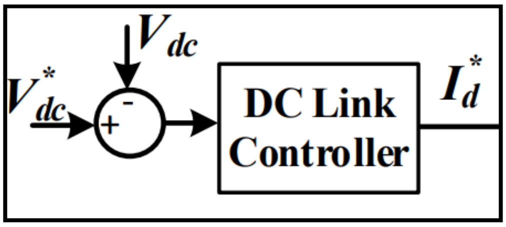

Figure A.14

Overview structure of the proposed VSG control system.

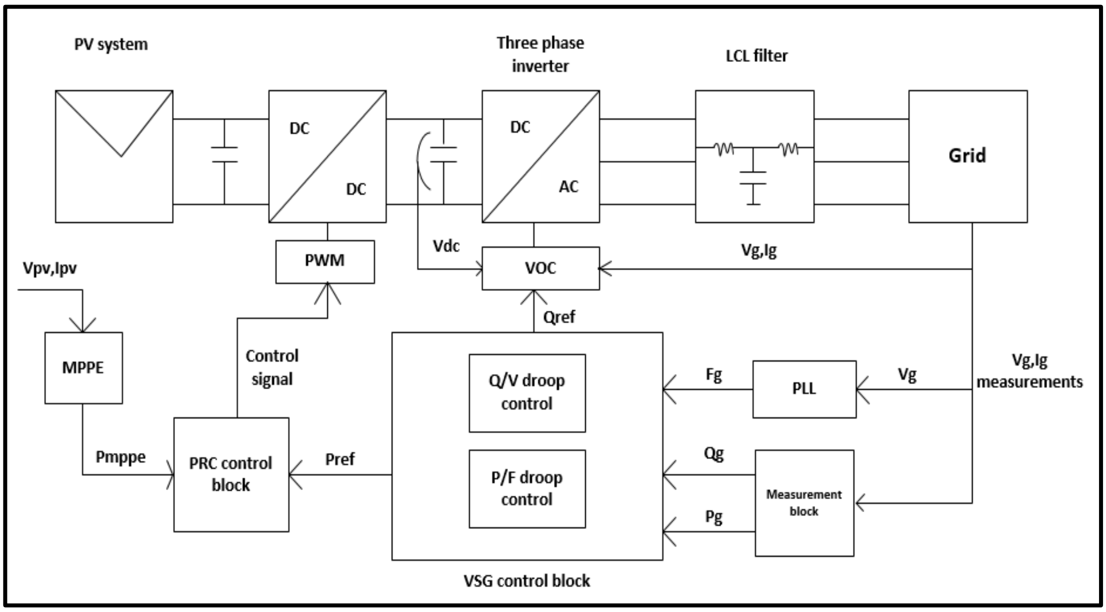

Figure A.15

Q-V droop control curve.

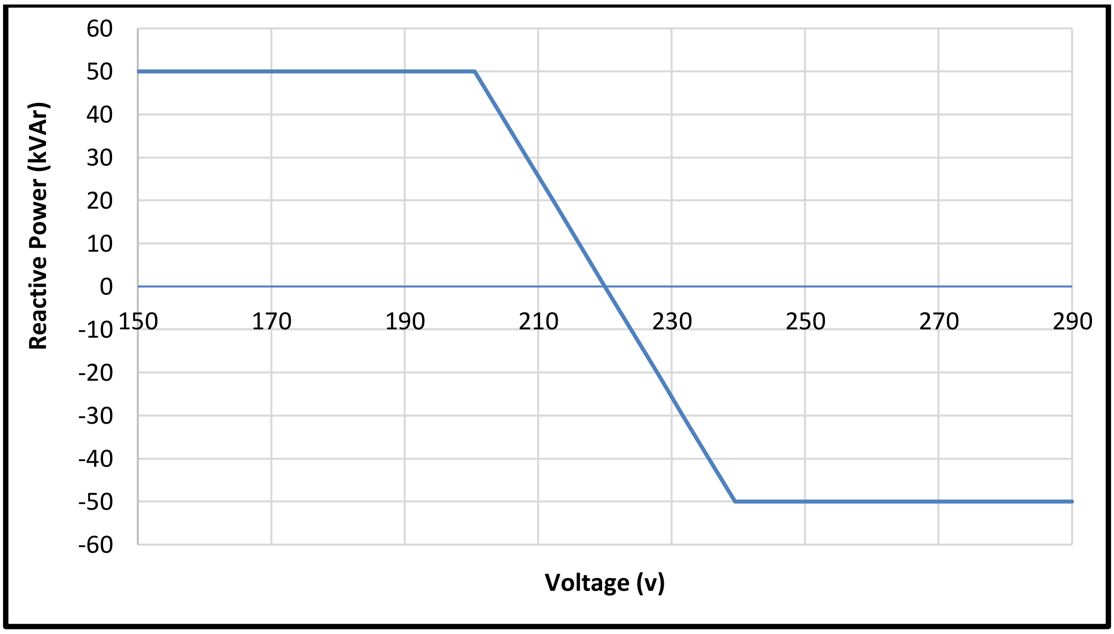

Figure A.16

P-V characteristic curve.

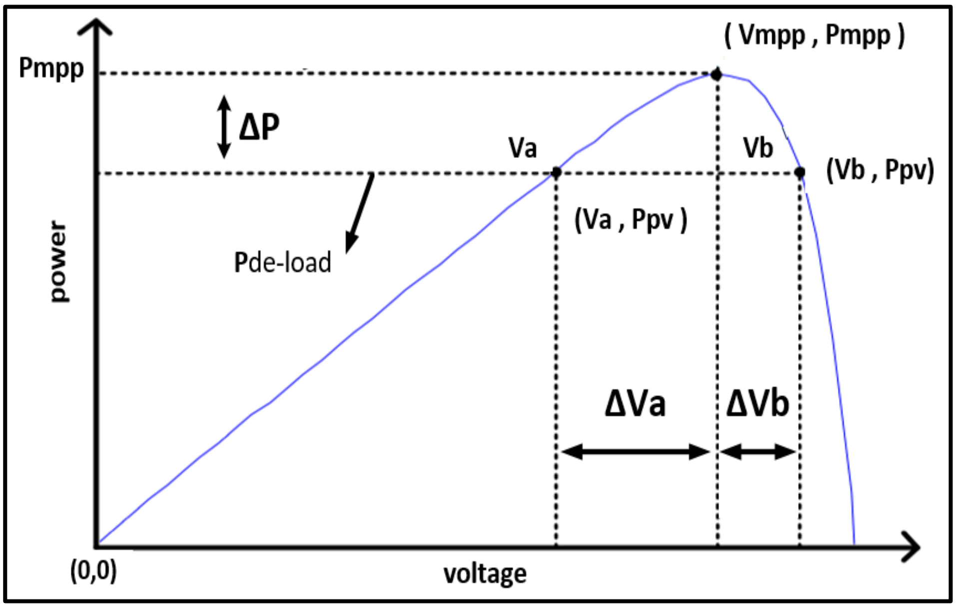

Figure A.17

The output power of PV in different solar radiations with 10% reserve power of $\boldsymbol{P_{mpp}}$ *[56].*

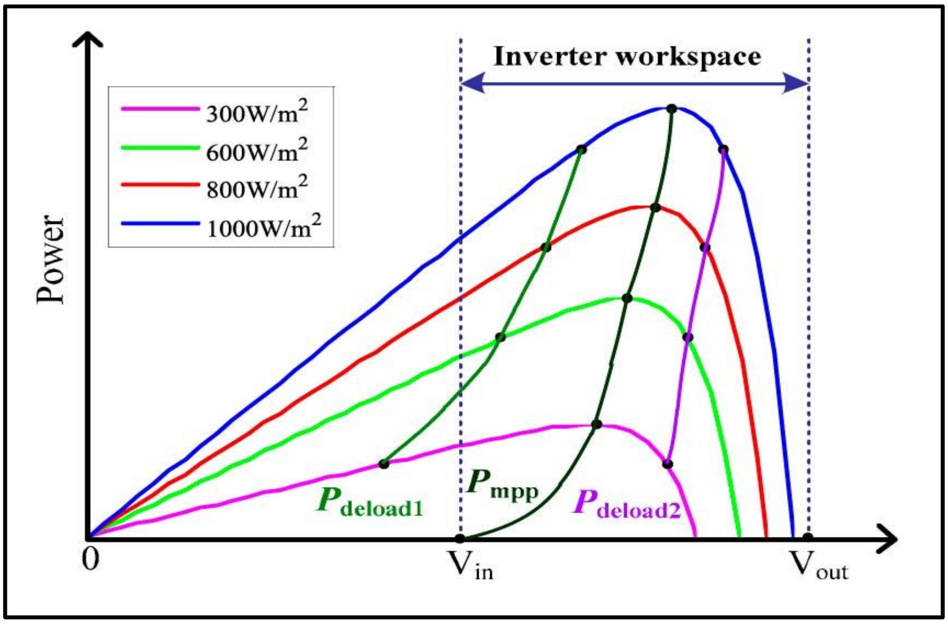

Figure A.18

Comparison between MPPT and PRC voltage.

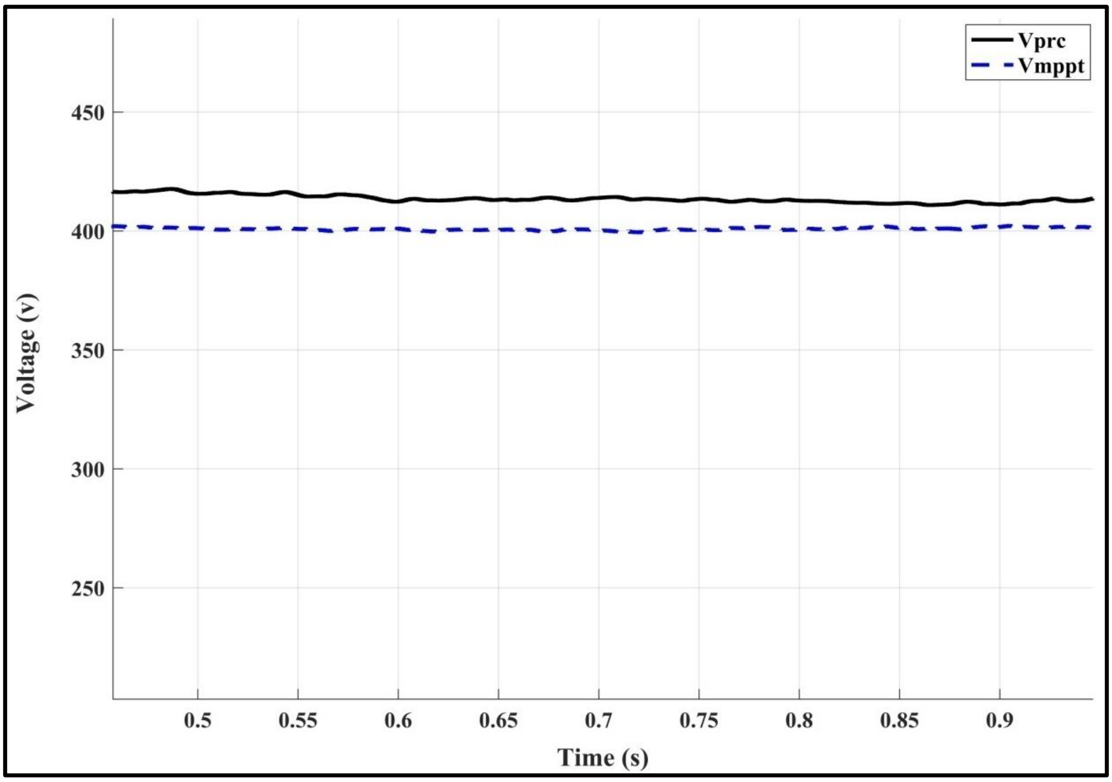

Figure A.19

Block diagram of PV with power reserve control.

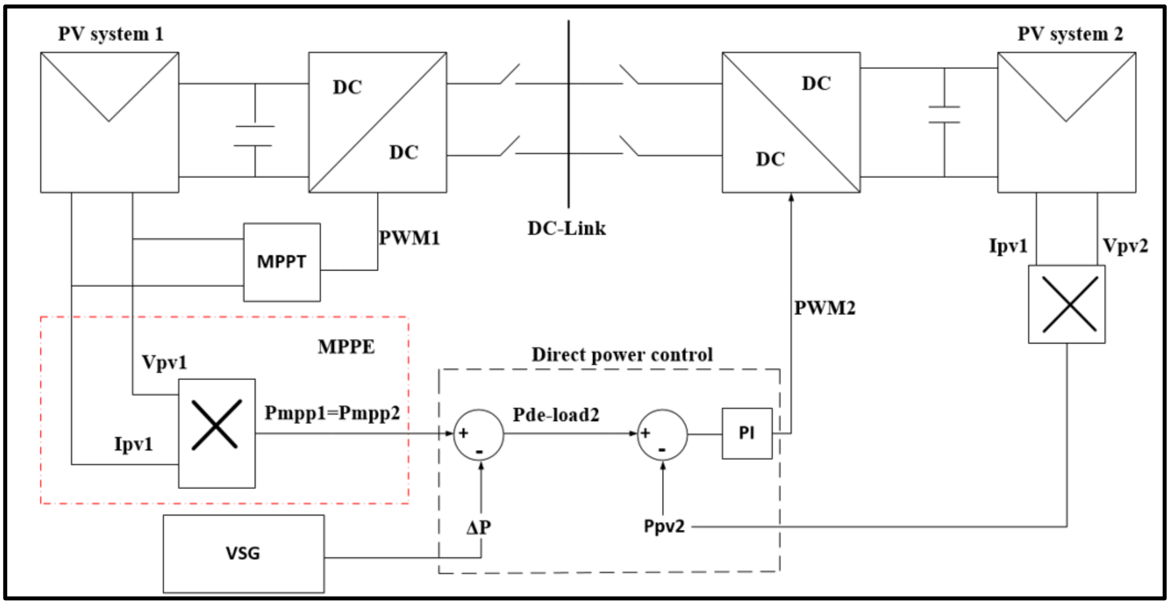

Figure A.20

P-F droop control curve.

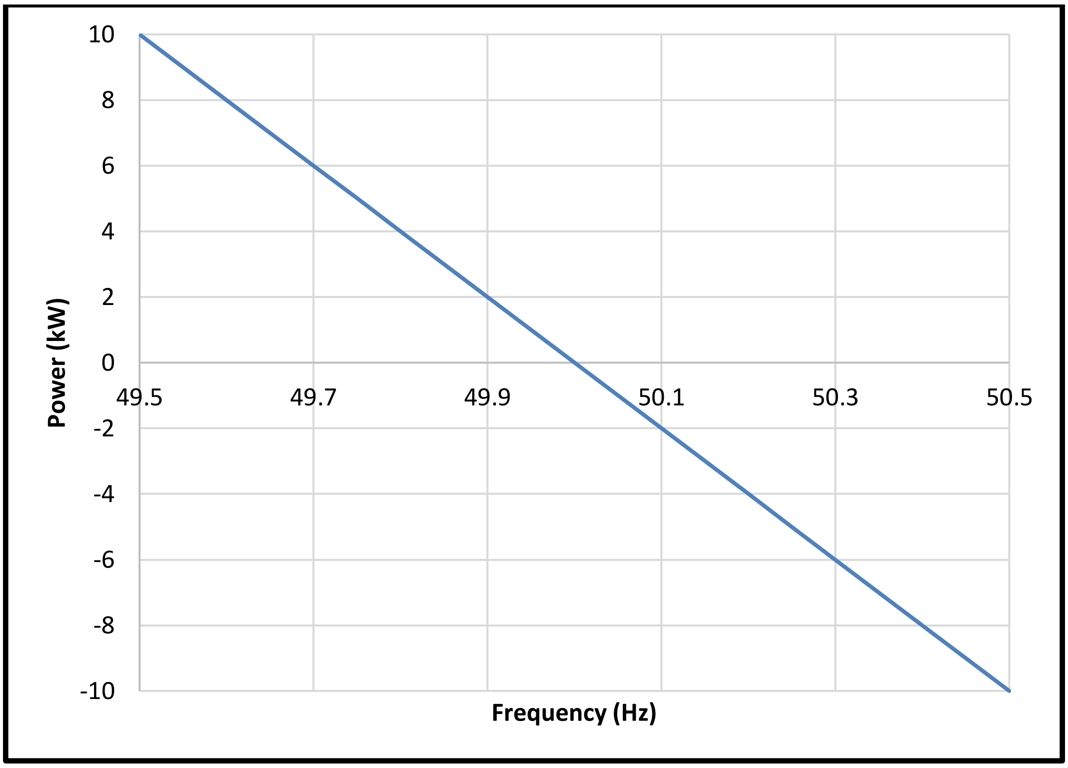

Figure A.21

The system structure for the first scenario.

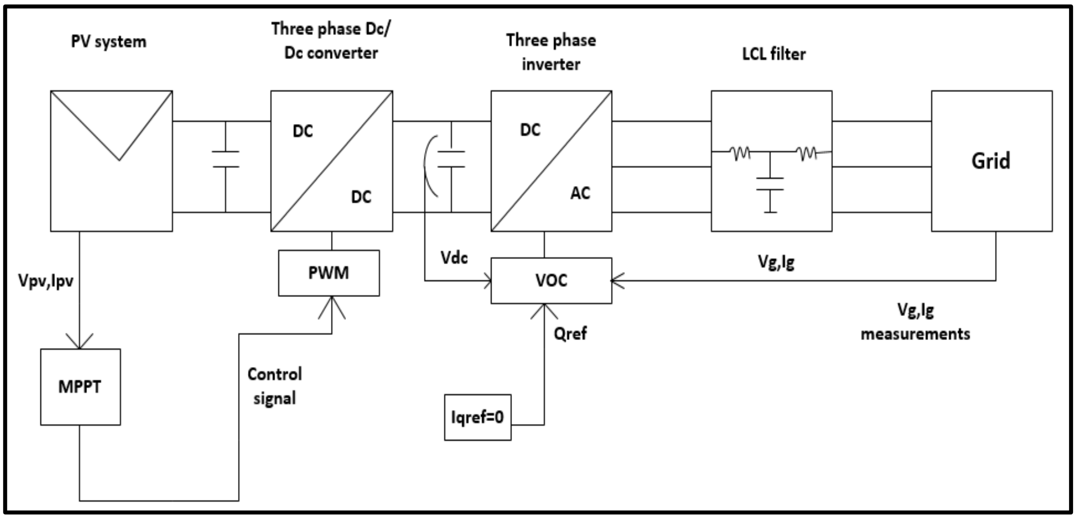

Figure A.22

Grid, Inverter, Load active (kW) and reactive (kVAr) power during the normal condition.

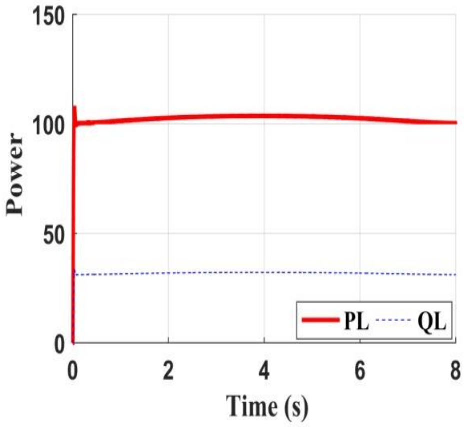

a− active and reactive load power.

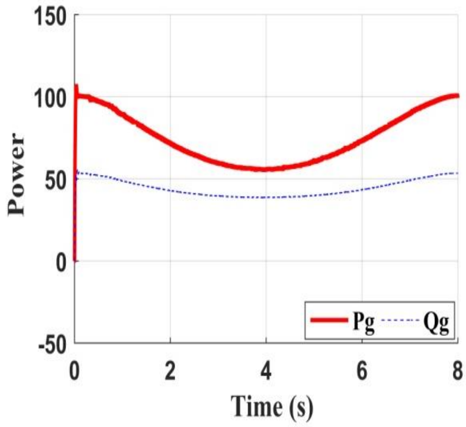

b− active and reactive grid power.

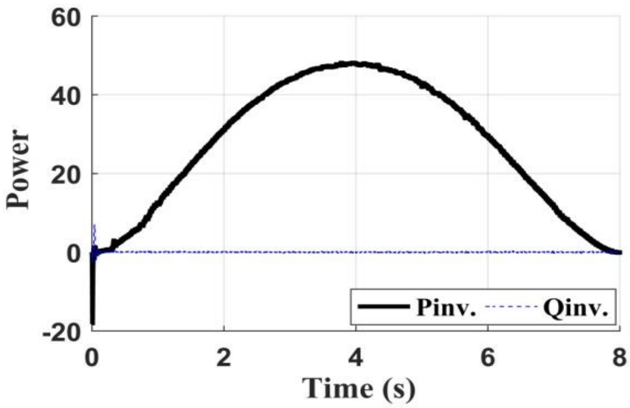

c− inverter output

Figure A.23

Load voltage (V) during the normal condition.

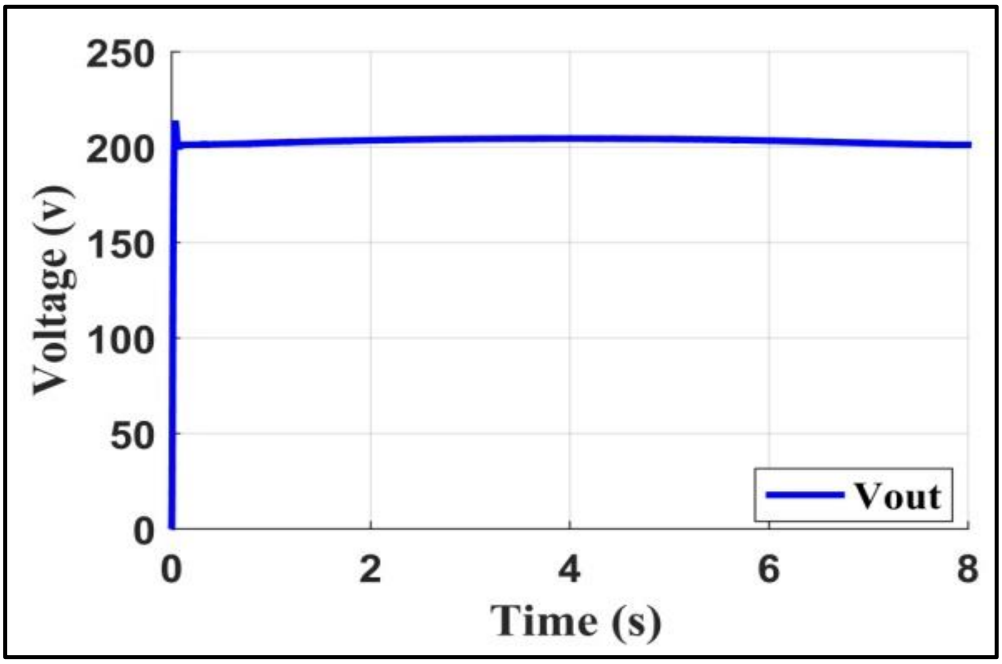

Figure A.24

Load voltage (V) during high and low PV power with low load.

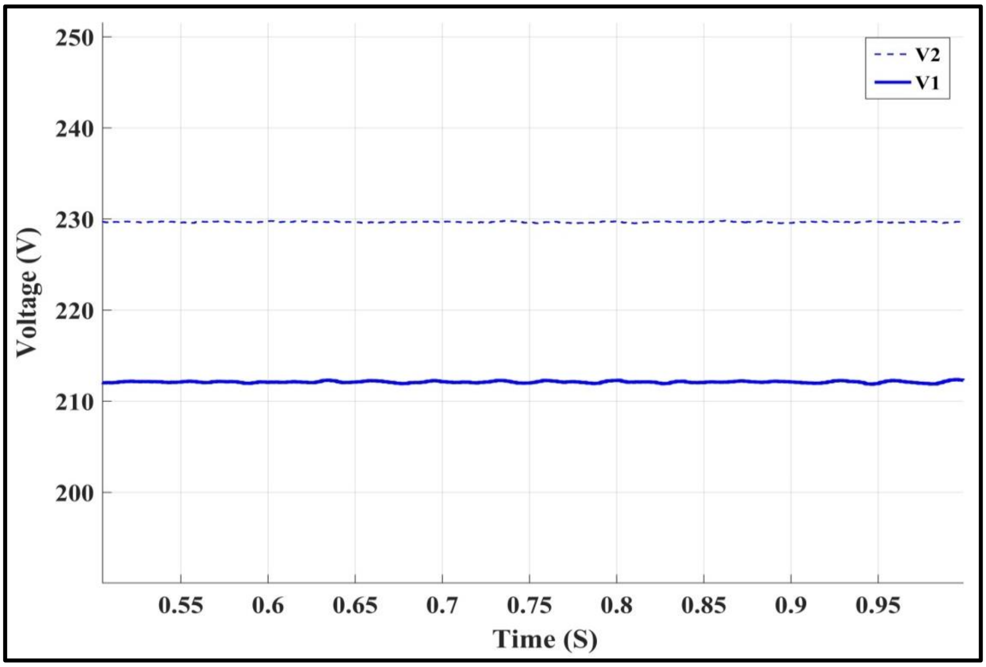

Figure A.25

Grid, Inverter, Load active (kW) and reactive (kVAr) power when the PV power more than the load power by using the MPPT control.

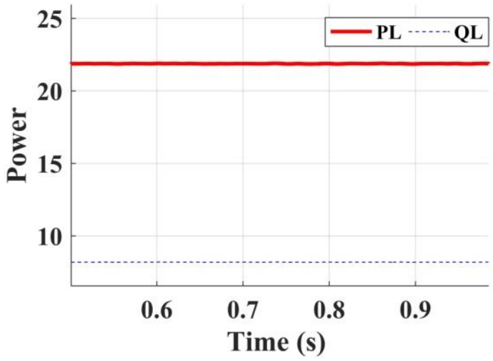

a– Active and reactive load power.

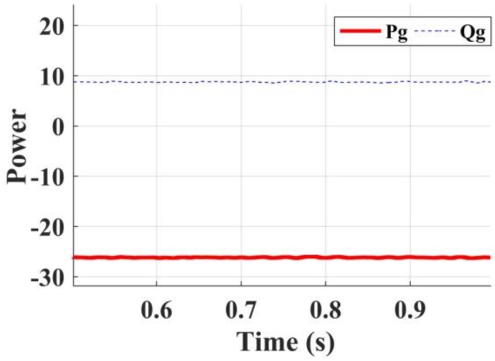

b– Active and reactive grid power.

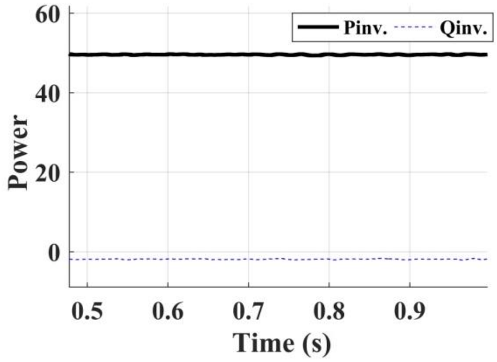

c– Inverter output.

Figure A.26

Load voltage (V) during low PV power with high load.

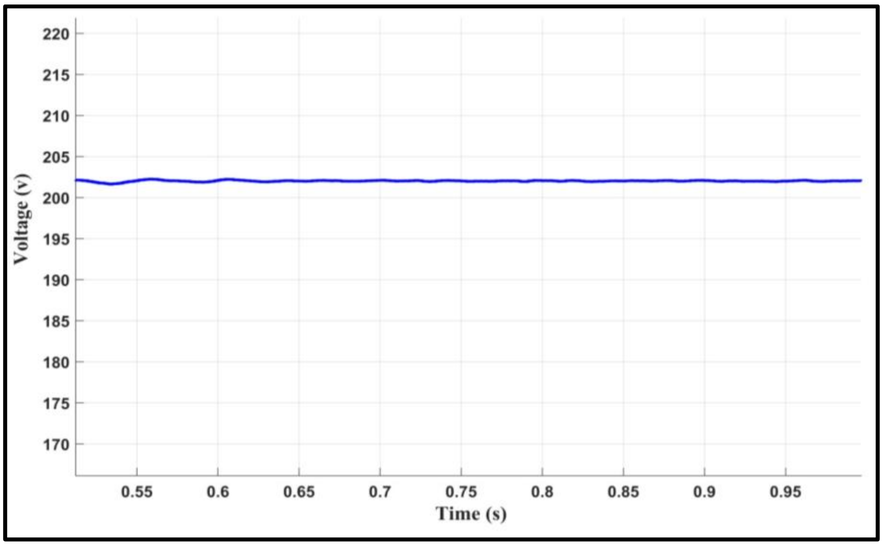

Figure A.27

Load voltage improvement (V) with low PV power.

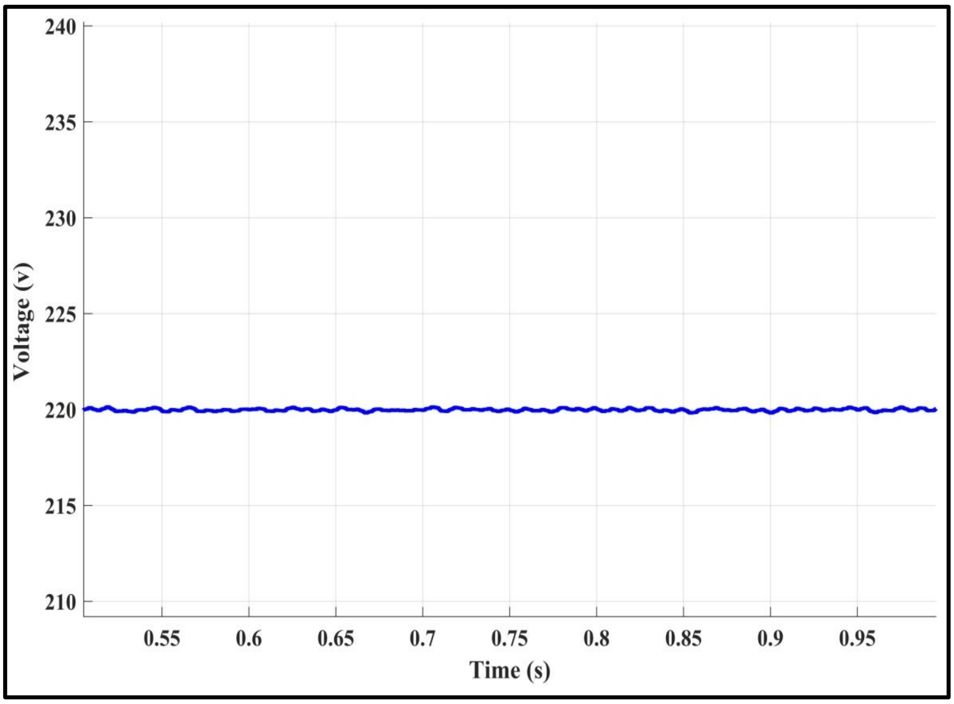

Figure A.28

Load voltage (V) before and after the improvement

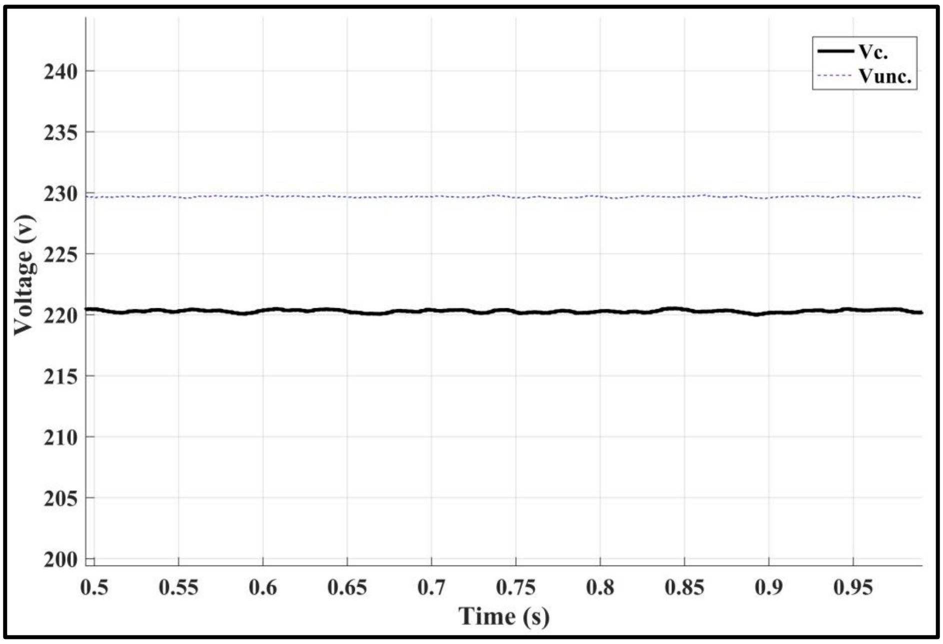

Figure A.29

Inverter, Load active (kW) and reactive (kVAr) power.

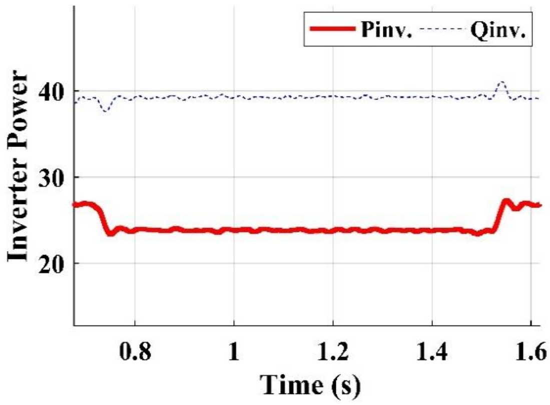

a- Inverter output with PRC control.

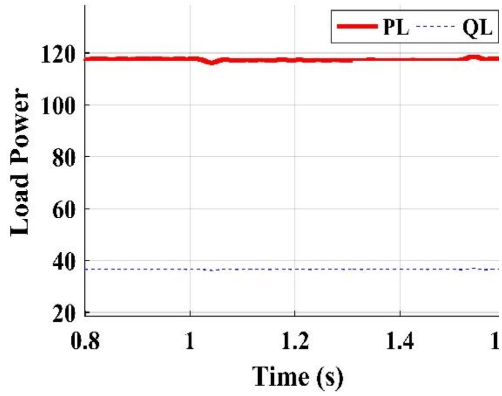

b− Active and reactive load power

Figure A.30

Reserve power and system frequency.

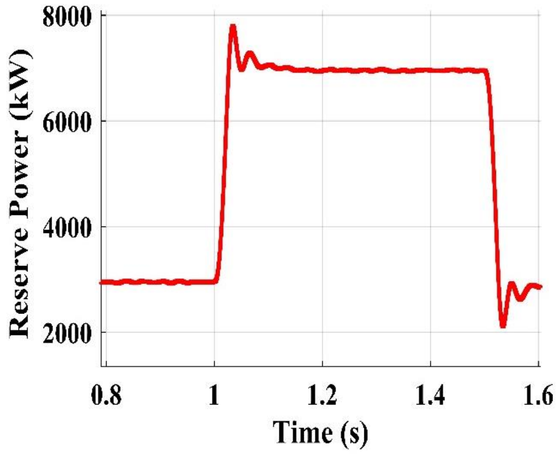

a- Reserve power (kW).

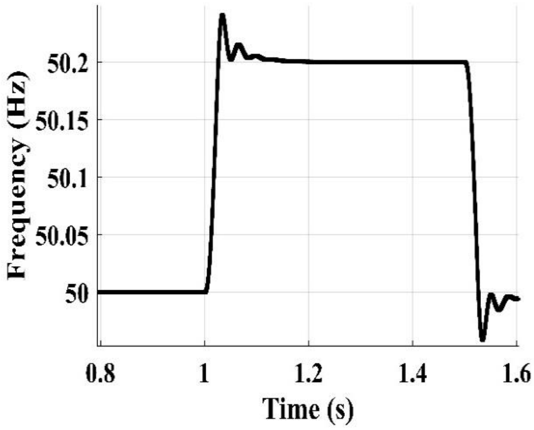

b- System frequency.

Figure A.31

Load voltage with and without using the proposed control strategy.

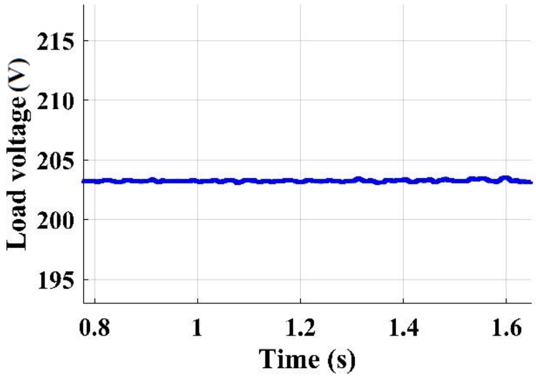

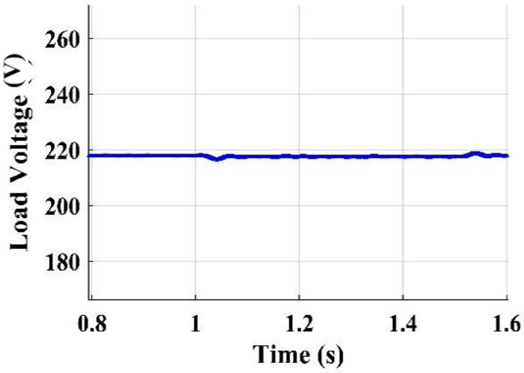

a- load voltage without control. b- load voltage with the proposed control.

جــامعـــة النجاح الوطنية

كليـــة الدراســـات العليـــا

إستراتيجية التحكم ومحددات التشغيل للعاكس الكهروضوئي الذي يدعم الشبكة الرئيسية بناءً على مفهوم المولد الافتراضي المتزامن

إعداد

نور الدين باسم محمد غزاوي

إشراف

أ.د. معين عمر

د. مروان محمود

قدمت هذه الأطروحة استكمالا لمتطلبات الحصول علي درجه الماجستير في هندسة القوى الكهربائية، من كلية الدراسات العليا، في جامعة النجاح الوطنية، نابلس– فلسطين.

2022

إستراتيجية التحكم ومحددات التشغيل للعاكس الكهروضوئي الذي يدعم الشبكة الرئيسية بناءً على مفهوم المولد الافتراضي المتزامن

اعداد

نور الدين باسم محمد غزاوي

إشراف

د. معين عمر

د. مروان محمود

الملخص

ازدياد مستوى محطات توليد الكهرباء المعتمدة على مصادر الطاقة المتجددة مثل الطاقة الشمسية وطاقة الرياح في الشبكة الكهربائية أدّى إلى ظهور مشاكل كبيرة تتعلق باستقراريه الشبكة الكهربائية وذلك بسبب طبيعة الطاقة المتغيرة الناتجة عن العوامل الجوية من اشعاع شمسي متغير و بسبب نقص او انعدام خاصية القصور الذاتي والتخميد في العواكس الكهربائية التي تستعملها. من جهة اخرى، يتم استخدام المولد المتزامن المتواجد في الشبكات الكهربائية في تحسين استقراريه النظام الكهربائي بسبب الخصائص التي يتمتع بها والتي تساعده على التحكم بجهد وتردد الشبكة.

هذه الأطروحة تقدم طريقة تحكم جديدة للمولد التزامني الافتراضي في العواكس الكهربائية دون استخدام أنظمة تخزين الطاقة الخارجية مثل البطاريات، حيث يتم استخدام القدرة الفعالة الاحتياطية والقدرة الغير فعالة المتاحة في العاكس الكهربائب لتحسين تردد وجهد الشبكة بدلاً. و مفهوم الطاقة الاحتياطية يمكن تطبيقه في سياق الشبكة الذكية لأن بعض العواكس الكهربائبة هي عواكس ذكية ذكية ويتم التحكم فيها جميعًا بواسطة وحدة تحكم. يمكن لمشغل الشبكة تقليل القدرة الناتجة من هذه العواكس في حالة زيادة القدرة المولدة من العواكس عن القدرة المطلوبة بواسطة الحمل. وفي الوقت نفسه ، يمكن تقليل أو زيادة القدرة الفعالة بدون الحاجة إلى استخدام وحدة تخزين خارجية بتكلفة استثمارية عالية.

تتضمن دراسة الحالة، العاكس الكهروضوئي بقدرة 50 كيلو فولت أمبير ، ونظام شمسي بقدرة 50 كيلو واط ، وجهد شبكة بمقدار 380 فولت. عندما يكون الإشعاع الشمسي 200 واط / م ^{2} ، وقوة الحمل 120kW, 37kVAr، يكون جهد الحمل 202.4 فولت. تعمل إستراتيجية التحكم المقترحة على تحسين الجهد بمقدار 17.6 فولت ليصبح 220 فولت.

عندما يكون الإشعاع الشمسي 1000واط / م^2 ، وقوة الحمل 20kW,7kVAr ، يكون جهد الحمل 230 فولت. يقلل التحكم المقترح من الجهد بمقدار 10 فولت ليكون 220 فولت، أما بالنسبة للتردد، يكون هنالك تردد متغير بمقدار ± 0.4 هرتز من التردد الاسمي البالغ 50 هرتز. يعمل التحكم المقترح على تحسين التردد بمقدار ± 0.4 هرتز ليكون 50 هرتز.

تم استخدام برنامج MATLAB / SIMULINK لمحاكاة وإظهار فعالية استراتيجية التحكم المقترحة لتحسين استقرار النظام مع سيناريوهات مختلفة.

الكلمات المفتاحية: المولد الافتراضي المتزامن، المولدات المتزامنة، استقرار الجهد الكهربائي، استقرار التردد، الطاقة الاحتياطية.